



# **Casing Coupling for Extreme Temperature Setting**

Haraldur Orri Björnsson

Thesis of 60 ECTS credits  
**Master of Science (M.Sc.) in Sustainable Energy  
Engineering**

September 2015





# **Casing Couplings for Extreme Temperature Setting**

Haraldur Orri Björnsson

Thesis of 60 ECTS credits submitted to the School of Science and  
Engineering  
at Reykjavík University in partial fulfillment  
of the requirements for the degree of  
**Master of Science in Sustainable Energy Engineering - ISE**

September 2015

Supervisor:

Dr. Einar Jón Ásbjörnsson,  
Professor, Reykjavík University, Iceland

Examiner:

Sverrir Þórhallsson  
Engineer, ISOR

Copyright  
Haraldur Orri Björnsson  
September 2015

# Casing Couplings for Extreme Temperature Setting

Haraldur Orri Björnsson

60 ECTS thesis submitted to the School of Science and Engineering  
at Reykjavík University in partial fulfillment  
of the requirements for the degree of  
**Master of Science in Sustainable Energy Engineering**

September 2015

Student:

---

Haraldur Orri Björnsson

Supervisor(s):

---

Dr. Einar Jón Ásbjörnsson

Examiner:

---

Sverrir Þórhallsson

The undersigned hereby grants permission to the Reykjavík University Library to reproduce single copies of this Thesis entitled **Casing Coupling for Extreme Temperature Setting** and to lend or sell such copies for private, scholarly or scientific research purposes only.

The author reserves all other publication and other rights in association with the copyright in the Thesis, and except as herein before provided, neither the Thesis nor any substantial portion thereof may be printed or otherwise reproduced in any material form whatsoever without the author's prior written permission.

.....  
date

.....  
Haraldur Orri Björnsson  
Master of Science

# Casing Couplings for Extreme Temperature Setting

Haraldur Orri Björnsson

September 2015

## Abstract

The next leap in utilization of geothermal energy for electricity production might comprise of drilling deep wells down to the roots of geothermal reservoirs. Near these roots fluid at very high temperature and even at supercritical conditions can be accessed. Extraction of such fluid from natural reservoirs can if some obstacles can be conquered revolve geothermal utilization and electricity production.

To allow deep geothermal wells to become a viable option a comprehensive research has to be carried out to eliminate all uncertainty regarding the resource. Furthermore the technical challenges which developers face on all stages from drilling and extraction to production have to be solved.

One of the most essential parts of a geothermal well is the casing, string of pipes which ensure the structural integrity of a well and seal the well from unwanted fluids from the geothermal reservoir. Successful casing design and installation increases the longevity of a well, while design or installation faults can render a well inoperable or be the cause of high maintenance cost. It has been identified that deep geothermal wells will test a casing string performance further than conventional wells and if deep geothermal wells are to be a feasible option the casing design has to be resilient and reliable.

This thesis reviews two threaded casing connection options proposed for extreme temperature settings and aims to answer which if any of examined options are best suited for deep wells of the future using finite element analysis. Assumptions made for the research are to some extent based on the Iceland Deep Drilling Project (IDDP).

The results indicate that conventional threaded options can't be recommended for examined conditions and premium connections with metal to metal sealing surface have no advantages over conventional connections under inspected loads. The results do not highlight any advantages of upgrading the casing to a higher grade material according to API 5CT standard.

# Fóðringatengi fyrir mjög heitar borholur

Haraldur Orri Björnsson

September 2015

## Útdráttur

Næsta stökk í jarðhitanýtingu til orkuframleiðslu gæti orðið borun á djúpum holum niður að neðri mörkum þess sem við skilgreinum sem jarðhitakerfi. Nærri þessum mörkum er að finna mjög heitann vökva, jafnvel við yfir-krítískt ástand sem getur að ýmsum skilyrðum uppfylltum bylt jarðhitanýtingu til raforkuframleiðslu.

Til þess að djúpholur verði raunhæfur kostur til orkuöflunar þarf bæði að rannsaka auðlindina, komast yfir alla óvissuþætti sem snúa að jarðhitakerfinu og ekki er síður nauðsynlegt að leysa tæknilegar áskoranir sem blasa við á öllum stigum frá öflun orkunnar til notkunar.

Á meðal mikilvægustu þátta í byggingu borholu eru fóðringar, rör sem meðal annars halda holunni heilli og skerma af vökva frá kaldari svæðum jarðhitageymis. Góð fóðringahönnun og vandaður frágangur auka líkur á góðri endingu borholu en gallar í hönnun og mistök við niðurstetningu geta valdið ótímabærri aflagningu holu eða háum viðgerðarkostnaði. Fyrir liggur að djúpholur gera kröfu um nýjar áherslur í fóðringahönnun og stór þáttur í að gera djúpboranir að raunhæfum möguleika er áreiðanleg fóðring sem getur staðist þá áraun sem, hitinn, dýpið og þrýstingurinn valda.

Í verkefninu er leitast við að svara hvort önnur þeirra tveggja tegunda fóðringatengja tengja sem skoaðar eru geti hentað í djúpholur framtíðarinnar. Rannsóknin var unnin með smábúta aðferð. Forsendur rannsóknarinnar voru mótaðar með íslenska djúpborunarverkefnið (IDDP) til hliðsjónar.

Niðurstöður leiða í ljós að ekki er hægt að mæla með hefðbundnum skráfuðum fóðringasamsetningum fyrir þær aðstæður sem hér eru skoðaðar og hágæða tengi með innbyggðum þéttifleti sem horft hefur verið til virðast ekki hafa kosti fram yfir hefðbundin skráfuð tengi. Niðurstöður benda einnig til þess að ekki sé ávinningur hvað tengingar varðar að velja fóðringar í hærri efnisflokki samkvæmt API 5CT staðli.



## **Acknowledgements**

The author would like to thank all those who helped in the development of this thesis in one way or other with advices, guidance and motivation.

Special thanks go to Indriði Sævar Ríkharðsson, Sturla Fanndal Birkisson and my supervisor Einar Jón Ásbjörnsson.

Last but not least I would like to thank my family for limitless support and assistance.

# Table of Contents

<b>LIST OF FIGURES.....</b>	<b>XI</b>
<b>1 INTRODUCTION .....</b>	<b>1</b>
1.1 THE PROJECT .....	1
1.2 THE AUTHOR AND HISTORY OF THE PROJECT .....	3
1.3 OBJECTIVE AND RESEARCH QUESTION .....	4
<b>2 BACKGROUND .....</b>	<b>5</b>
2.1 GEOTHERMAL ENERGY .....	5
2.2 HISTORY OF GEOTHERMAL ENERGY UTILIZATION .....	6
2.2.1 <i>Utilization of high temperature geothermal resources.....</i>	<i>7</i>
2.2.2 <i>Conventional geothermal well design.....</i>	<i>9</i>
2.3 THE DEEP DRILLING PROJECT .....	11
2.3.1 <i>Super-critical conditions in a geothermal reservoir.....</i>	<i>11</i>
2.3.2 <i>General overview of IDDP.....</i>	<i>12</i>
2.3.3 <i>IDDP-1.....</i>	<i>13</i>
2.3.4 <i>IDDP-2.....</i>	<i>15</i>
2.4 CASING OPTIONS.....	17
2.4.1 <i>Standards .....</i>	<i>17</i>
2.4.2 <i>Steel and its behavior under load.....</i>	<i>17</i>
2.4.3 <i>Von Mises yield criteria.....</i>	<i>21</i>
2.4.4 <i>Casing for high temperature setting.....</i>	<i>22</i>
2.4.5 <i>Connections.....</i>	<i>23</i>
2.5 CASING LOADS.....	26
2.6 CASING FAILURE MODES.....	28
2.6.1 <i>Failure mechanism.....</i>	<i>28</i>
2.6.2 <i>Collapse .....</i>	<i>28</i>
2.6.3 <i>Burst.....</i>	<i>29</i>
2.6.4 <i>Connection failure .....</i>	<i>29</i>
2.6.5 <i>Fatigue failure.....</i>	<i>30</i>
<b>3 METHODS.....</b>	<b>31</b>
3.1 THE RESEARCH METHOD .....	31
3.2 FINITE ELEMENT ANALYSIS (FEA).....	32
3.2.1 <i>Discrete system, general solution.....</i>	<i>34</i>
3.3 MODELING OF THE CONNECTION.....	37

3.3.1	<i>The material</i> .....	38
3.3.2	<i>Model and meshing</i> .....	40
3.3.3	<i>ANSYS model setup and constraints</i> .....	41
3.3.4	<i>Load case 1</i> .....	42
3.3.5	<i>Load case 2</i> .....	43
3.3.6	<i>Load case 3</i> .....	44
<b>4</b>	<b>RESULTS</b> .....	<b>45</b>
4.1	RESULTS FOR CONNECTION TYPE 1, GRADE K55.....	45
4.1.1	<i>Load case 1, API BTC, K55</i> .....	45
4.1.2	<i>Load case 2, API BTC, K55</i> .....	51
4.2	RESULTS FOR CONNECTION TYPE 2 (PROPRIETARY CONNECTION), GRADE K55 .....	52
4.2.1	<i>Load case 1, premium connection, K55</i> .....	52
4.2.2	<i>Load case 2, premium connection, K55</i> .....	59
4.3	RESULTS FOR CONNECTION TYPE 1, API BTC, GRADE L80 .....	61
4.3.1	<i>Load case 1, API BTC, L80</i> .....	61
4.3.2	<i>Load case 2, API BTC, L80</i> .....	62
4.4	RESULTS FOR CONNECTION TYPE 2 (PROPRIETARY CONNECTION), GRADE L80.....	63
4.4.1	<i>Load case 1, Proprietary connection, L80</i> .....	63
4.4.2	<i>Load case 2, proprietary connection, L80</i> .....	64
4.5	CASING STRING IN PRETENSION .....	67
4.5.1	<i>Pretension, API-BTC, K55</i> .....	67
4.6	COMPARISON, CONVENTIONAL CONDITIONS.....	69
<b>5</b>	<b>CONCLUSIONS AND DISCUSSIONS</b> .....	<b>70</b>
5.1	CONCLUSIONS.....	70
5.2	DISCUSSIONS .....	71
<b>6</b>	<b>BIBLIOGRAPHY</b> .....	<b>73</b>

## List of figures

Figure 1: History of geothermal utilization in Iceland [7].	7
Figure 2: Lindal diagram, potential energy utilization depending on temperature [4].	8
Figure 3: Conventional geothermal casing program [2].	10
Figure 4: Well IDDP-1 As built [12].	14
Figure 5: IDDP-2 well design, [13].	16
Figure 6: Stress-Strain diagram.	19
Figure 7: Conventional API BTC coupling [19].	23
Figure 8: Proprietary connection.	25
Figure 9: The model and section.	37
Figure 10: Assumed properties of K55 casing material.	39
Figure 11: Assumed properties of L80 casing material.	39
Figure 12: The model mesh, proprietary connection.	41
Figure 13: The boundary conditions.	42
Figure 14: Thermal load, case 1.	43
Figure 15: Thermal load, case 2.	44
Figure 16: Load 1, API BTC $t=0$ .	46
Figure 17: Load 1, API BTC $t=250$ .	46
Figure 18: Load 1, API BTC $t=750$ .	47
Figure 19: Load 1, API BTC $t=1250$ .	47
Figure 20: Load 1, API BTC $t=1500$ .	48
Figure 21: API BTC, K55, reactive axial force, load 1.	49
Figure 22: API BTC, pipe end deformation, load 1.	50
Figure 23: API BTC, K55, reactive axial force load 2.	51
Figure 24: Load 1, Proprietary connection $t=0$ .	52
Figure 25: Load 1, Proprietary connection $t=250$ .	53
Figure 26: Load 1, Proprietary connection $t=750$ .	53
Figure 27: Load 1, Proprietary connection $t=1250$ .	54
Figure 28: Load 1, Proprietary connection $t=1500$ .	54
Figure 29: Load 1, Proprietary connection sealing surface $t=0$ .	55
Figure 30: Load 1, Proprietary connection sealing surface $t=250$ .	55
Figure 31: Load 1, Proprietary connection sealing surface $t=750$ .	56

Figure 32: Load 1, Proprietary connection sealing surface $t=1250$ .....	56
Figure 33: Load 1, Proprietary connection sealing surface $t=1500$ .....	57
Figure 34: Load 1, Proprietary connection, K55, reactive axial force. ....	58
Figure 35: Load 1, Proprietary connection, K55, sealing surface contact pressure. .....	58
Figure 36: Load 2, Proprietary connection, K55, reactive axial force. ....	59
Figure 37: Load 2, Proprietary connection, K55, sealing surface contact pressure. .....	60
Figure 38: Load 2, Proprietary connection, K55, sealing surface gap. ....	60
Figure 39: Figure 40, API BTC, N80, reactive axial force, load 1. ....	61
Figure 41: API BTC, N80, reactive axial force, load 2.....	62
Figure 42: Proprietary connection, L80, reactive axial force, load case 1.....	63
Figure 43: Proprietary connection, L80, sealing surface contact pressure.....	64
Figure 44: Proprietary connection, L80, reactive axial force, load case 2.....	64
Figure 45: Proprietary connection, L80, sealing surface contact pressure, load case 2. ....	65
Figure 46: Proprietary connection, L80, sealing surface gap. ....	66
Figure 47: API-BTC, K55 in tension when thermal load is applied. ....	67
Figure 48: API-BTC, K55, pretension and neutral when thermal load is applied.	68
Figure 49, Comparison, Premium connection axial force. ....	69

# **1 Introduction**

## **1.1 The project**

The latest potential addition to the Icelandic energy resource base is extraction of supercritical fluids from natural hydrothermal resource for electricity production.

High temperature geothermal resources have been exploited for electricity production for decades and in 2000 the Iceland Deep Drilling Project (IDDP) was established by three Icelandic energy companies, Orkuveita Reykjavíkur (OR), Landsvirkun (LV), HS Orka (HS) and the National Energy Authority of Iceland (OS). The IDDP is a research and development project with the objective to improve the economics of geothermal resources, minimize the environmental impact of harnessing geothermal resources and support sustainable development [1].

In order to explore the deep sections of the hydrothermal systems the IDDP has drilled, and will in near future drill, deep geothermal wells into the roots of a geothermal system in order to extract high temperature and even supercritical fluids. Supercritical fluids are expected to be found below 3-3,5 km depth [1]. If the IDDP project will be a success it might increase the energy resource base in Iceland significantly and bring geothermal utilization to the next level. If supercritical fluid from natural resources can be extracted, an order of magnitude higher energy output can be expected per well, compared to conventional high temperature geothermal wells assuming same volumetric output which is mainly a result of higher pressure.

Utilization of high temperature geothermal resources is a puzzling task which demands highly developed technical solutions. Majority of geothermal drilling practices and well design methods are derived from the oil drilling industry but special measures have to be taken to adapt the methods and techniques to the high temperatures and pressures of a high temperature geothermal environment. The conditions anticipated in deep geothermal wells are far more extreme than in a conventional high temperature geothermal system. The expected extreme

pressure and temperature conditions require various aspects of well and casing design to be reconsidered so that well integrity can be ensured.

The most critical part of a geothermal well is the casing, 3-5 strings of concentric steel pipes that span from the surface to the bottom of the well. The outermost casing string is short while the innermost casing string extends into the reservoir. The casing prevents loose material from blocking the hole, provides anchorage for the wellhead, isolates the well from the surroundings and surroundings from the well, counters losses of drilling fluid during drilling and protects the well and formation from fracturing and breakdown [2]. The innermost casing string serves also as a conductor for the extracted fluid. If a geothermal well is to be successful, a resilient casing is an essential part. A casing failure can restrict flow from a well and in worst case render the well inoperable or even cause a steam eruption outside the well.

The casing string is generally made of 10-13 meter long members that are connected with threaded couplings. Various casing materials are available as well as coupling types but none of these options are explicitly engineered for extreme temperature conditions prompted by supercritical fluids which are to be extracted from deep geothermal wells. The casing connection is the weakest part of the casing string and majority of all casing failures in oil wells in operation are coupling failures [3]. The casing material and couplings have to be chosen to sustain the load prompted by the extreme conditions expected in deep geothermal well.

In this thesis the load history of a casing string in a high temperature well will be explained, casing connection and material options will be reviewed and a finite element analysis on two threaded casing connection options for extreme temperature conditions will be presented.

## **1.2 The author and history of the project**

This project is the final thesis of the author's MSc degree in Sustainable Energy Engineering at the Reykjavík University.

The author has since 2004 when he started working on geothermal drilling rigs been interested in drilling technology, drilling methods and development in geothermal utilization. Therefore the master's thesis was a great opportunity to dig deeper into this field and this project was an easy choice.

The initial plan was to simulate downhole conditions and perform a mechanical experiment on casing couplings under restricted thermal expansion. This plan was abandoned since sample material and sufficient funds were not available to complete the research with appropriate equipment in a laboratory.

When it became clear that the initial plan could not be accomplished a new scope was defined. Similar research as planned in the initial proposal was carried out but different methods were used. The mechanical experiment was substituted for a finite element analysis research but the goal was the same, to examine connection options for extreme temperature setting in a deep geothermal well.

It is the author's hope that the findings of this project can somehow contribute to future development in deep geothermal drilling.



### **1.3 Objective and research question**

The main objective of this case study is to review and examine casing connection options for extreme temperature setting. Expected reservoir conditions and drilling plans of the IDDP are widely referred to in this project.

The study is carried out using finite element analysis in order to answer the question; ***which, if any, of the casing material and connection options examined are best suited for a deep geothermal well?***

## 2 Background

### 2.1 Geothermal energy

According to the International Geothermal Association (IGA) geothermal energy is literally the heat contained within the earth but is generally used to indicate the recoverable and exploitable part of the heat [4]. Geothermal energy is found to some extent everywhere on the planet but high temperature reservoirs, hot, permeable and porous enough for efficient electricity production are scarce and primarily associated with volcanic regions.

A geothermal gradient, which is a heat gradient, can be used to define the heat potential of geothermal systems. The geothermal gradient  $^{\circ}\text{C}/\text{km}$  expresses the increase in temperature with depth. The average geothermal gradient on earth is little less than  $30^{\circ}\text{C}/\text{km}$  but in active geothermal areas the values are substantially greater. In the Icelandic geothermal literature, reservoir temperature at 1 km depth has been used to classify geothermal resources. In order to be classified as high temperature geothermal resource the temperature at 1 km depth has to be  $200^{\circ}\text{C}$  or greater while systems with temperatures lower than  $150^{\circ}\text{C}$  at 1 km depth are referred to as low temperature geothermal systems [5].

The earth consists of two main layers and a core. The crust is the outermost layer with a thickness of roughly 30-50 km on the continental plates but only 5-10 km on the oceanic plates. The second layer, the mantle, is a little less than 3 km thick and in the center of the earth is the core which has a diameter of 7000 km.

The geothermal heat source is the internal heat of earth, mainly produced by decay of radioactive elements in the mantle and the core but also primordial heat from the original formation of earth. Active geothermal areas are found where the internal heat can ascend easily through the core to surface. Those areas are in general on tectonic plate boundaries and near volcanoes. The Mid Atlantic Ridge, a divergent tectonic plate boundary along the Atlantic Ocean through Iceland is an example of geothermally active tectonic plate boundary while the geothermal system in Hawaii is a volcanic hotspot far from tectonic plate boundaries.

The energy transfer medium, which transfers the geothermal energy to the surface is water and the exploitable high temperature geothermal systems are therefore called hydrothermal systems. To be ideal for energy extraction the heat alone is not enough. The hot formations have to be porous and permeable enough to contain water and allow flow through the system.

If all conditions are favorable, wells can be drilled into porous and permeable layers of a geothermal system and fluid extracted for energy production. The energy can either be used directly for heating or indirectly for electricity production.

## **2.2 History of geothermal energy utilization**

Geothermal systems have been used for bathing, washing and cooking for thousands of years. But even though geothermal energy is an integral part of everyday life in Iceland, and many other parts of the world today, energy production only started in the early 1900's [6].

Utilization of the geothermal resource was until in the early 1900's limited to the superficial part of the resource, but the development has progressed fast in the last 100 years. The first geothermal power plant in the world was established in Lardarello, a small village in Italy, and the first geothermal plant in Iceland, Bjarnarflag Power Station, went online in 1969.

Since then, 5 geothermal power plants have been constructed in Iceland and a few more are on the horizon.

Geothermal energy became an essential part of the Icelandic culture when district heating systems were installed around the country. The district heating systems generally harness the low temperature part of the resource though high temperature steam is used to heat water for the capital city and surroundings in Nesjavellir and Hellisheiði, are co-generation plants with combined heat and electricity production. The geothermal electricity production in Iceland is limited to the high temperature resource.

Today major part of primary energy use is from geothermal and it accounts for 25 % of the electricity production in Iceland. [7]

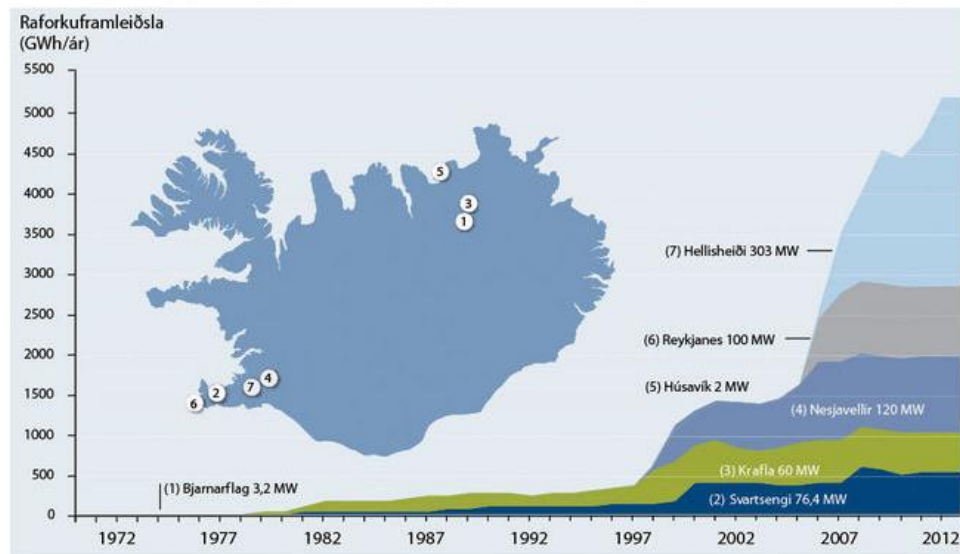


Figure 1: History of geothermal utilization in Iceland [7].

### 2.2.1 Utilization of high temperature geothermal resources

High temperature geothermal resources are primarily exploited for electricity generation, though co-generation, simultaneous production of heat and power is a feasible option in many areas which can yield economic and environmental benefits.

The electricity is either produced by converting thermal energy to mechanical energy in a conventional steam turbines or in binary plants. In conventional steam turbine the heat energy is converted into mechanical energy as the steam expands through the turbine. The steam enters the turbine at high pressure and expands to lower pressure in the turbine. The velocity of the steam increases as it expands and the steam gains kinetic energy. As the steam passes the rotor blades of the turbine the kinetic energy is converted to mechanical rotational energy which drives a generator.

Geothermal turbines are either non-condensing back-pressure units where the steam expands to atmospheric pressure or condensing turbine units where the steam expands to a condenser where the pressure is lower than atmospheric pressure. The condensing unit can produce approximately twice the energy from the same steam quantity at same temperature and pressure compared to backpressure unit.

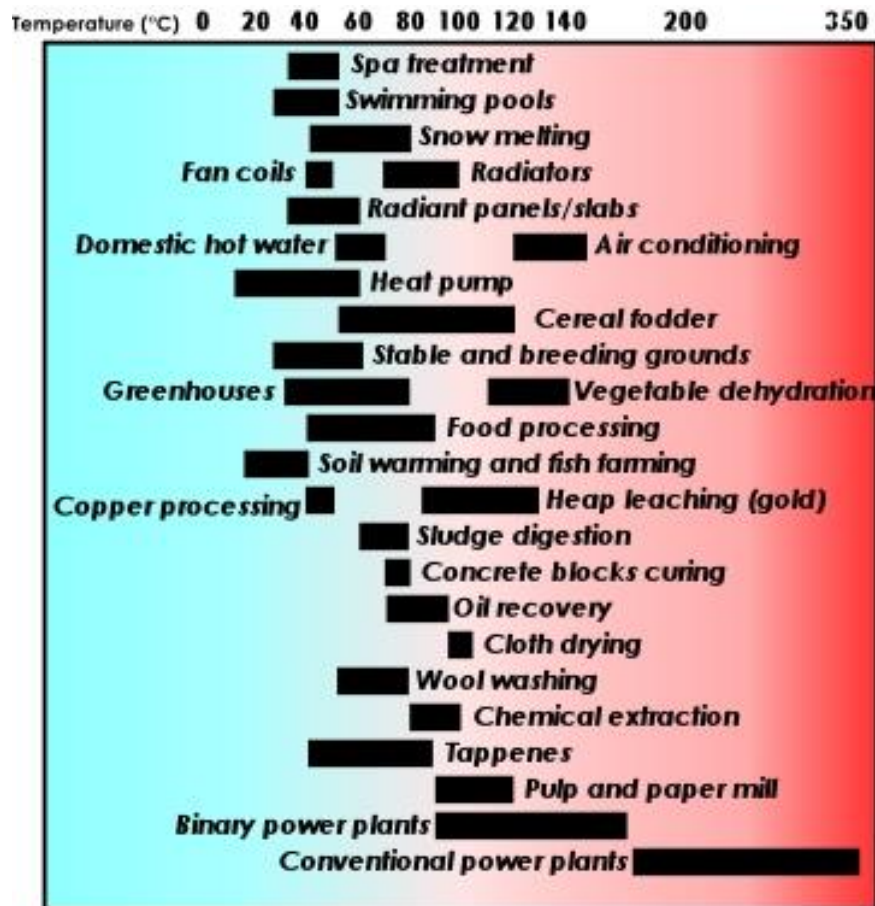


Figure 2: Lindal diagram, potential energy utilization depending on temperature [4].

In a binary plant the working fluid which acquires heat from the geothermal fluid is circulated in a closed loop. Binary plants are commonly used for lower temperatures and where the geothermal fluid has some harmful properties. Binary plants have also been installed as addition to conventional flash plants for increased efficiency [8].

The potential power output of a geothermal power plant is mainly a function of two variables; the mass flow of geothermal fluid and the energy content

(enthalpy) of the fluid. The enthalpy is a function of the reservoir temperature and pressure and therefore not in control of the developer. The other main variable, the maximum mass flow can be controlled to some extent by the operator by the number of wells drilled into the reservoir.

### **2.2.2 Conventional geothermal well design**

Geothermal wells extend from surface into the geothermal reservoir. Wells are drilled in few stages, each cased with a separate string of steel pipes (casing strings) which are firmly cemented from bottom to surface. The first step has the greatest diameter and the last step is the slimmest. Each casing string has certain purpose. The most important factors are to ensure structural integrity of the well, both during the drilling process and in operation, and to ensure fluids are contained within the well, drilling fluids and geothermal fluids. Each casing string also provides support and anchorage for next stage wellhead [2].

In a conventional well the first casing, apart from the surface conductor, is the surface casing which prevents loose material from near surface from collapsing into the hole while drilling.

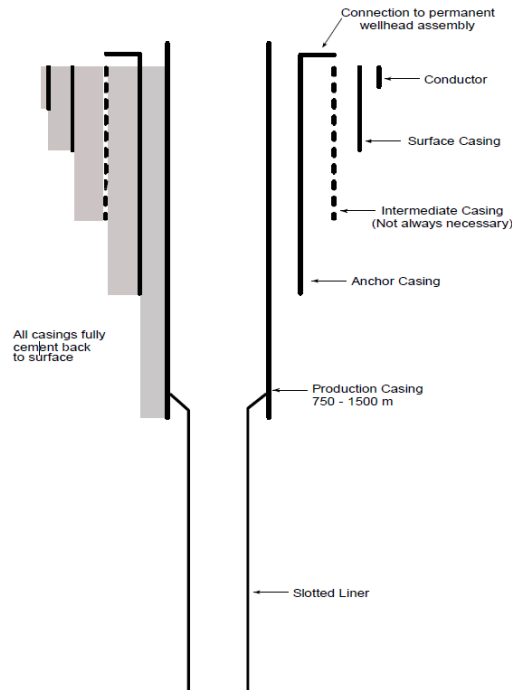


Figure 3: Conventional geothermal casing program [2].

The second casing string, the anchor casing, is usually an anchor for the permanent wellhead and has to be able to enclose fluid at high temperature and pressure.

The last cemented casing string is the production casing which serves as a conductor for the geothermal fluid. The setting depth of this casing string is based on expected pressure and temperature at the bottom of the well, the overburden pressure or fracture pressure at the casing shoe has to be greater than the fluid pressure expected from well bottom. For the upper casing strings, the overburden pressure at the casing shoe has to be greater than expected fluid pressure at depth of the particular section. This measure is taken to ensure that any fluid flows up the casing rather than out into the formation around.

All the casing strings mentioned above are cemented from bottom to surface and are therefore fixed. The last string of pipes that is installed into the well is the liner. The liner is a slotted or holed casing pipe which is installed into the production section of the well, the open hole section. The liner is either standing on the bottom of the well or hanging inside the production casing.

## **2.3 The deep drilling project**

### **2.3.1 Super-critical conditions in a geothermal reservoir.**

Under normal conditions it is quite easy to identify phases of water since the thermodynamic properties of water and steam phases are very different.

The properties of water are mainly a function of pressure and temperature. Although the chemical content of the fluid plays a role the first two variables are dominant.

The properties of liquid water are approximately constant from zero to evaporation temperature. At boiling point, properties change and become different from the properties of the liquid phase. After vaporization the properties change with respect to temperature and pressure.

The specific volume of the steam phase is roughly 1000 times the specific volume of the liquid phase at atmospheric pressure. This example indicates how different the properties are. At the critical point the thermodynamic properties of the water phase and the steam phase are indistinguishable, the boundaries between the vapor and liquid phases are no longer present [9]. The critical point occurs above 374°C and 220.6 bar respectively for water but higher for saline seawater [10]. In a liquid dominated reservoir those conditions are to be expected from a depth of around 3.5 km.

A conventional high temperature geothermal system cycle is a convection cycle where a cold recharge is heated down in the reservoir by contact with hot reservoir rock. Upwards flow of hot liquid is driven by buoyancy forces. On top the reservoir is isolated by an impermeable cap.

Water in liquid dominated geothermal reservoirs generally follows a boiling point curve. The boiling point restricts the maximum temperature inside a liquid dominated reservoir but magmatic intrusions can disturb this hydrostatical equilibrium at shallower depth than the critical point is expected [10].



Heat increases with depth but for supercritical fluid to exist in a geothermal reservoir, permeability and porosity need to be sufficient at the depth of the critical point and below. At a certain temperature and depth there is a transition zone where the rock goes from being brittle to ductile. This change creates a critical boundary in a geothermal system where heat is introduced to the system with conduction. Below this transition zone that begins at 500-600°C in a basaltic system but at 370-400°C in a rhyolitic system permeability is likely diminishing. From the depth of the critical point and down to the conductive boundary layer (CBL) supercritical fluid up to 600°C is expected to be found [11].

Yet supercritical fluid from natural resources have not been utilized for energy production but recently attempts have been made by the IDDP project. Supercritical fluid has higher enthalpy and increased buoyancy near the critical point can increase mass and energy extraction potential.

### **2.3.2 General overview of IDDP**

It has been estimated that for the same volumetric steam flowrate, a well producing from naturally occurring supercritical geothermal reservoir can generate power output, magnitude higher than a conventional geothermal well due to higher wellhead pressure. This increased energy output can potentially be accomplished without increasing the environmental footprint. If exploitable supercritical fluids can be extracted in an economically viable way it can support sustainable development and expand the Icelandic energy portfolio significantly.

The IDDP is a long term project, run mutually by the government and the energy industry. The IDDP was established in 2000 and nine years later the world known IDDP-1 well was drilled in Krafla and when this is written the IDDP-2 in Reykjanes has been designed and proposed.

The drilling of wells into supercritical zones offers many challenges, the construction of the well tests the limit of high end equipment and utilization of the liquid is not straightforward. The hostile environment requires conventional methods to be adapted to expected conditions.

### 2.3.3 IDDP-1

Drilling of the well IDDP-1, which was initially designed to be drilled down to 4500 meter depth, was initiated in 2008 and stopped in the summer of 2009 at 2096 meters after a series of incidents which happened following intersection of magma.

The well was designed to produce steam from a supercritical reservoir and the wellhead pressure was expected to exceed 220 bar. The well is therefore designed with two intermediate casings and a wellhead according to pressure class ANSI 2500 [12].

The first casing string of the original design is a welded 32" surface casing to 100 meter depth followed by two intermediate casing strings, the first one 24 ½" to 300 meter depth and the second intermediate casing string, 18 ⅝" to 800 meters.

The anchor casing which supports the wellhead was designed to consist of two types of casing pipes, a 13 ⅝" 88,2 lb./ft., grade T95 to 300 meter depth and a 13 ⅜" 72 lb./ft., grade K55 to 2400 meters.

The production casing was designed to be a 9 ⅝", 53,5 lb./ft. grade K55 and set depth was to be 3500. The well design can be described as an extended or a stretched version of conventional well. Same principles are followed but an additional intermediate casing is added and heavier pipes used compared to conventional wells in order to improve the pressure barrier. The first three casing strings were set close to planned depth but due to stability problems the anchor casing was set to 2000 meter depth rather than the planned 2400 meters.

Though the well did not reach final planned depth it has been considered a partial success.

The well has since it was opened produced highly superheated steam and it has been concluded that extraction of fluids near a magma body is possible [12].

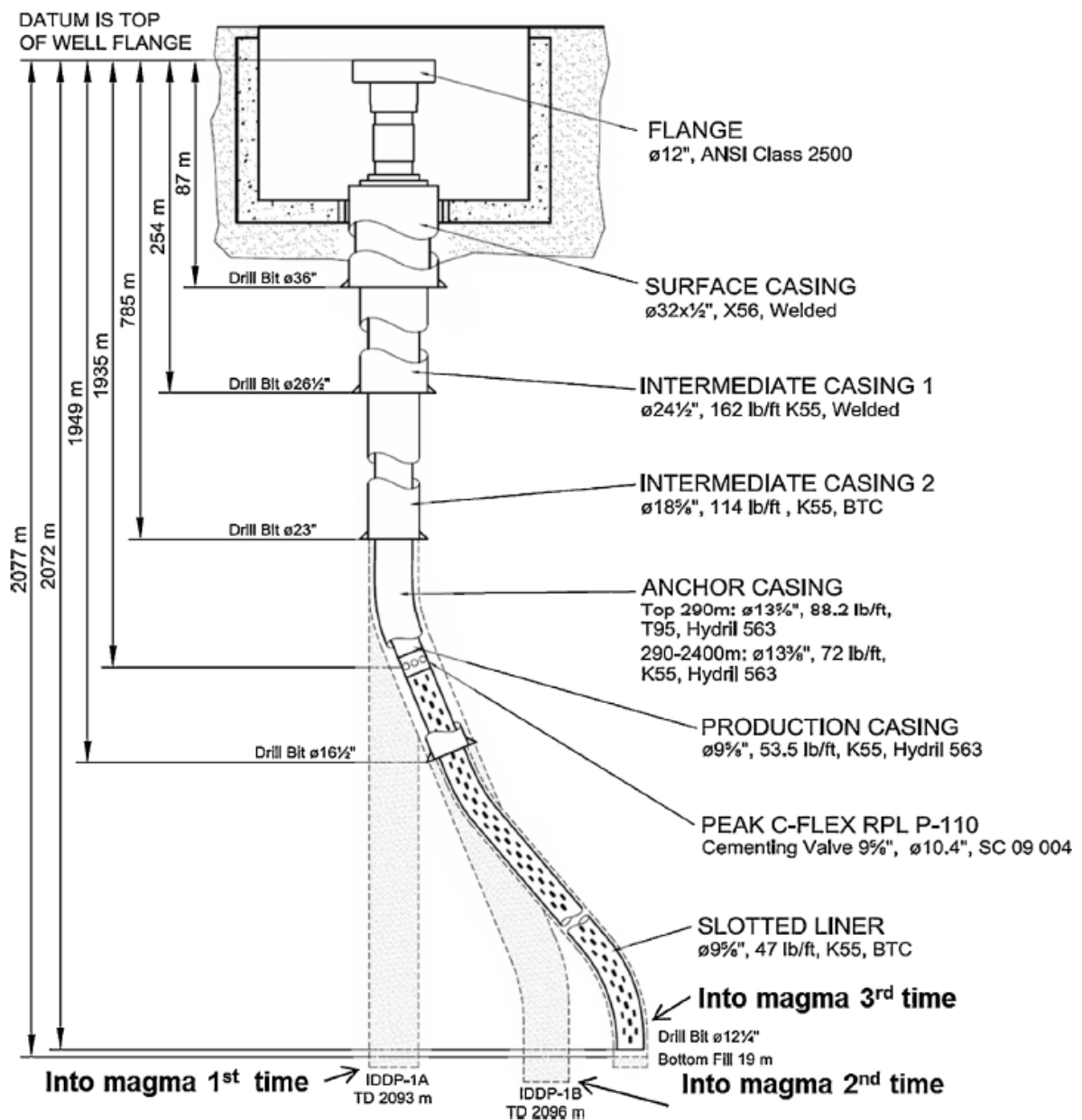


Figure 4: Well IDDP-1 As built [12].

#### **2.3.4 IDDP-2**

The proposed location for the second well IDDP-2 is at Reykjanes, near Reykjanesvirkjun, a geothermal power-plant developed by HS-Orka. The location is in the vicinity of wells that have already been drilled and are connected to the plant. This is both an advantage and a challenge. The formations are relatively well known, as well as the geothermal system down to 2700 meters, but the challenge is that the deep well has to be properly isolated from the upper production zone of the reservoir [13].

The main difference between IDDP-1 and the proposed IDDP-2 is that the upper part of the geothermal system at Reykjanes contains saline water and the supercritical point is therefore expected at greater temperature and therefore at greater depth than in Krafla where IDDP-1 is located.

If a geothermal reservoir is in hydrostatic equilibrium and boiling from surface the critical point is reached around 3500 meter depth, 375°C and 220 bar in a fresh water dominated reservoir while in a sea-water dominated reservoir, critical conditions are expected at a depth around 4600 meters, 411°C and 300 bar. If the reservoir temperature and pressure follow boiling point depth curve below the already explored 3000 meters the critical point in Reykjanes can't be expected above 5000 meter depth but intrusions can possibly be found at shallower depth similar to the ones opposed in Krafla [13]. Localized superheated or supercritical zones can be anticipated in the vicinity of shallow intrusions like described earlier.

In general the suggested design for IDDP-2 is identical to IDDP-1, the main modification is that setting depths have been altered to suite the site and the proposed design suggest one intermediate casing rather than two. The single most important proposed alteration to the design which concerns the scope of this thesis is that API BTC couplings are proposed for the production casing instead of wedged Hydrill couplings. The wedged couplings offer better seal at high temperature setting than the API BTC and the producer claims this type has greater tensile strength than conventional options. The experience from IDDP-1 is

that this particular coupling type did not perform better than conventional couplings and the production casing does not have to be completely gas tight [13].

A few innovative well design options were considered for IDDP-2. Among those options are connections which allow expansion and do not transfer stress, material with low thermal expansion and a hanging casing which is free to expand. Still technical difficulties, availability of material and high cost have caused conventional design and material use to come on top.

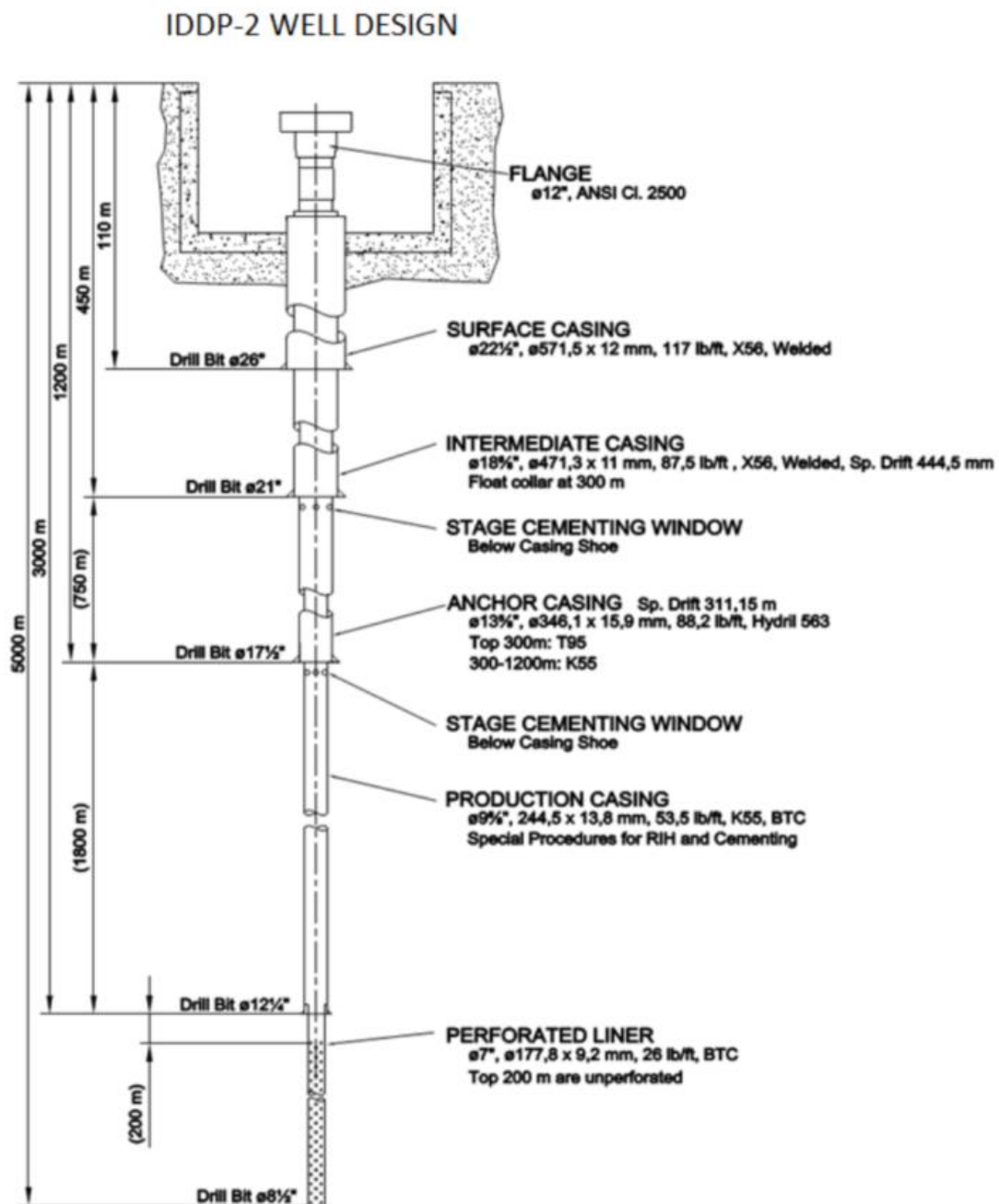


Figure 5: IDDP-2 well design, [13].

## **2.4 Casing options**

### **2.4.1 Standards**

Unlike the petroleum industry the geothermal industry has no undisputed standard organization which covers all materials, equipment and operating procedures [14].

The petroleum industry has developed equipment and operating standards and as the geothermal industry has derived methods from the oil drilling industry the standards have been used extensively for geothermal well design. The leader in this field has been the American Petroleum Institute (API). Several other standards are used by the geothermal industry, for example, ISO the ASME boiler and pressure vessel code and The New Zealand Code of Best Practice.

API-5CT specifies steel pipes for use as casing or tubing for wells. The standard specifies delivery conditions for steel pipes and couplings. It specifies manufacturing process, material requirements, dimensions, masses tolerances, defects and marking.

Casing for most of geothermal wells in Iceland, including IDDP has been manufactured according to API standards. This thesis will refer to the API-5CT standard for casing and tubing regarding casing physical characteristics and material properties.

### **2.4.2 Steel and its behavior under load**

Steel is a hard tough metal composed of iron, alloyed with small percentage of carbon and various other metals. Steel is and has been one of the main construction materials used and is the preferred material for well casing. Steel is in all comparison a low cost alloy of high strength. According to ASM, the American Society for Metals, steel is an important material because of tremendous flexibility in metal working and heat treating to produce a wide variety of mechanical, physical and chemical properties [15].

Steels properties are not just dependent on the ingredients. The microstructure can be influenced and the material properties altered by heat treatment where the steel is heated and cooled in a controlled environment in order to modify structure and manipulate hardness, strength ductility and elasticity.

Manufacturing process and treatment for each grade is carefully outlined for each casing grade in API-5CT along with upper and lower limit for all additives. Steel is an elastic material which follows a linear stress-strain path to the yielding point according to Hooke's law;

$$F = k * X$$

Where F is the acting force, X is the displacement and k is a stiffness constant. The Hooke's law states that for relatively small deformation of an object the displacement is directly proportional to the deforming force. The stress is;

$$\sigma = \frac{F}{A}$$

Where  $\sigma$  is the stress, F is the acting force and A is the cross sectional area of the material. The strain is;

$$\epsilon = \frac{\Delta L}{L}$$

Where  $\epsilon$  is the strain, L is the length of the material in the direction of the force and  $\Delta L$  is the elongation.

The slope of the stress-strain relationship in the elastic region represents the stiffness of the material which is defined by the modulus of elasticity, most often referred to as Young's modulus E;

$$E = \frac{\sigma}{\epsilon}$$

If a material is under axial load the material will elongate in the direction of the load. In the elastic region the volume of the material is constant and when the length of the material increases there must be a contraction in the material

perpendicular to the elongation axis for this argument to hold. The relationship between the transverse and axial strain is the Poisson's ratio. Poisson's ratio can be expressed as;

$$\mu = \frac{\epsilon_{transverse}}{\epsilon_{longitudinal}}$$

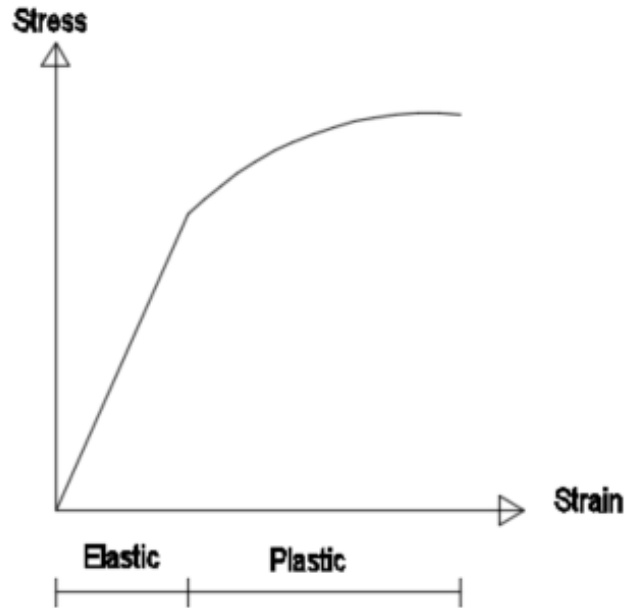


Figure 6: Stress-Strain diagram.

In the range, below the yield point within the elastic limit, steel can deform when load is applied and return back to original state when the load is relaxed. In other words, the material behaves like a spring which is stretched or compressed and returns back to the original state when the load is relaxed. If the stress exceeds the yield strength, the material deforms plastically. If the deformation is plastic the material will not return to its original shape and the deformation is permanent. When the forces applied make the stress in the material exceed the yield strength the elongation of the material is no longer proportional to the increase in stress and the material does not behave elastically and plastic deformation occurs. If material is deformed plastically the shape of it is altered and the micro structure of the material.



The microstructure of metals consist of grains which consist of unit cells in which atoms are arranged in a particular order. The cell structure repeats throughout the volume of the grains which are called crystallites. The structure is called lattice in which atoms are placed at lattice points within the material [16]. In a stress free state the atoms are in their equilibrium positions. Plastic deformation involves breaking of atomic bonds, movement of atoms and restoration of atomic bonds.

Strain hardening is a metal hardening process which involves plastic deformations. When a metal is deformed plastically, irregularities and dislocations within the crystal structure of the material are moved and new are created. The more dislocations within a material the more it becomes tangled. Lower mobility of the dislocations yields a stronger more brittle material. This process must happen at temperatures low enough for the atoms not to be able to rearrange them-selves. Strain hardening can drastically lower fatigue resistance of steel.

An important feature of steel, thermal expansion, is of exceptional significance to the matter discussed in this thesis. Steel like most other material expands in all directions with increased temperature and contracts with decreased temperature. Atoms that make a material are constantly vibrating. Increased heat makes the atoms of the material vibrate faster. As the atoms move faster the space that separates them increases and the object expands.

For many materials the thermal expansion is linear. This applies to steel. The linear thermal expansion is described by;

$$\Delta l = \alpha * l_0 * \Delta t$$

Where  $\alpha$  is the coefficient of thermal expansion,  $l_0$  is the initial length of the material,  $\Delta t$  is the temperature difference and  $\Delta l$  is the linear expansion of the material.

### 2.4.3 Von Mises yield criteria

The von Mises yield is used in this thesis to describe the behavior of the casing material.

The criteria is commonly used by engineers as a stress criteria. Material is then considered to yielding when von Mises stress exceeds the yielding point. Normal axial stress criteria can be used as a failure criteria but for complex multi-axial loads the von Mises theory has been recognized as more resilient and reliable.

The von Mises yield criteria is often referred to as a distortion energy theory since it states that yielding occurs when the distortion strain energy per unit volume exceeds the distortion strain energy per unit volume for yield in simple tension or compression of same material [17]. In other words, yield occurs when the distortion energy per unit volume equals the distortion energy in the same volume stressed to yield point axially.

According to Bickford [18], homogenous material can sustain high hydrostatic stresses without yielding. This leads to the assumption that plastic failure is associated with the difference between the actual stress and the hydrostatic stress.

In a three dimensional object the multiple stress can be combined to a single equivalent von Mises stress expressed by;

$$\sigma' = \left[ \frac{(\sigma_x - \sigma_y)^2 + (\sigma_y - \sigma_z)^2 + (\sigma_z - \sigma_x)^2}{2} \right]^{1/2}$$

#### **2.4.4 Casing for high temperature setting**

The most important pipe characteristics for a geothermal well casing are diameter, steel grade, weight, collapse resistance and internal yield pressure.

The API casing grade is a classification for minimum strength and performance of casing materials. Manufacturing process, chemical composition and requirements for tensile strength and hardness are specified in the standard for each grade. The API-5CT standard defines 11 grades for casing material [19]. The grades are denoted with a letter and a number. K55 is a common grade for geothermal application, 55 stands for the minimum yield strength, 55000 psi. The letter indicates manufacturing process, chemical composition and heat treatment. The details stated with the letter are further specified in the standard. Steel from two of the 11 grades defined in API-5CT were used for IDDP-1 and the same grades are proposed for well IDDP-2, T95 and K55 [13].

The welded surface casing in IDDP-1 and the proposed IDDP-2 is of grade X56 which is specified in API-5L specification for line pipe. Steel from grade L80 has also be considered for the next phase of the IDDP project. Higher grade steels, T95, P110 and Q125 offer far greater tensile strength and can tolerate higher internal pressure but the lower grade steel is selected for the production casing and liner. Lower grade milder steel is not as sensitive for exposure to hydrogen as hydrogen embrittlement prevents the use of high strength steel in high temperature geothermal wells since exposure to  $H_2$  and  $H_2S$  is inevitable. The way to avoid this is to select softer steel grades for high temperature geothermal environment [20].

For IDDP-1, the top part of the anchor casing was designed for creep and rupture but the rest of the casing for conventional conditions, burst and collapse resistance [21]. The T95 casing was used for the top 300 meters of the anchor casing in the IDDP-1 for higher burst resistance than K55. The top part of the anchor casing is not firmly cemented and must withstand the internal pressure and temperature expected at wellhead [22].

#### 2.4.5 Connections

As stated before the casing is an assembly of numerous 10-13 meter long pipes that are connected with a weld or a threaded coupling. There are many types of couplings available on the market but the most common connection type for geothermal wells standardized by API-5CT are API buttress (API BTC) thread connections.

The API BTC connection has a trapezoidal shape which can sustain higher axial loads than the API round thread [14]. Neither API BTC nor API rounded thread couplings have a machined metal to metal sealing surface but are sealed by tapered shape and thread compound.

Though API BTC threads are proven highly rated type of connection which has been installed into large number of wells, research have shown that the seal limit for this type of connection is 200°C [23].

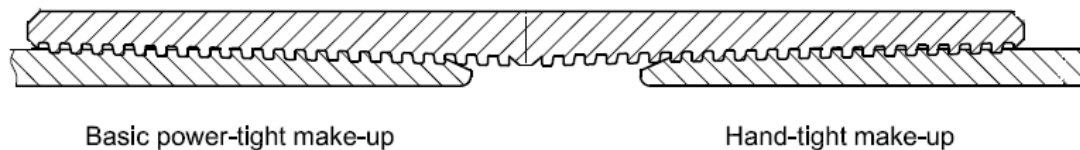


*Figure 7: Conventional API BTC coupling [19].*

Recent rapid development in the oil and gas industry has encouraged casing connection development. Deeper wells, horizontal wells and thermal wells demand more advanced coupling solutions than earlier shallower and simpler well designs. All new connections that have some advantages over traditional connections go by the name premium or proprietary connections. Those advantages can be better sealing, easier makeup, higher tensile strength, smaller outer diameter etc.

The oil and gas industry is the biggest player on the casing market, hence products and testing methods have been fitted to the industries requirements and needs.

Loads on casing couplings in oil and gas wells is well within the elastic limit of the material but the great loads from restrained thermal expansion in a geothermal

well can, and most often does surpass the elastic limit of the casing and the coupling.

Enhanced oil recovery technique, thermal recovery (TR), where steam is injected into the oil reservoir has recently become a common method for oil extraction. This method generates downhole conditions which has much in common with inhospitable conditions faced in a high temperature geothermal well, cyclic thermal loads and high casing stress due to restricted thermal expansion. The main difference is that the conditions in a TR well are fully controlled by the operator.

As the market share of proprietary connections grew the necessity to standardize and classify products and testing protocols to guarantee quality and reliability of such connections became great. API-5C5 addresses structural and material performance of proprietary connections as well as ISO-13679 which is identical.

Proprietary connections with machined metal to metal sealing surfaces are amongst those new connections. Connections of this kind have many advantages over the traditional API BTC and API round. The metal to metal premium connections are easier to make up, provide better seal and can't be over-torqued easily.

Conventional connections are made up to a triangular stamp on the pipe body. Both ends of the casing and the connection are cut in a taper and when the end of the pipe and the coupling are in full contact the edge of the coupling matches a triangular mark on the pipe. If the connection is tighten past this position the pipe end is compressed and the coupling expands which increases stress on both the pipe and connection and can decrease the connections rigidity. The tools, used on the rigs for the assembly, are powerful and extreme care is required when the connections are made up. Proprietary connections with metal to metal seal surface are far less vulnerable to damage from aggressive make up.

Casing coupling efficiency is defined in the Drilling Data Handbook [24] as the ratio of the critical cross-section of the connection to the steel pipe body cross-section expressed in percentage.

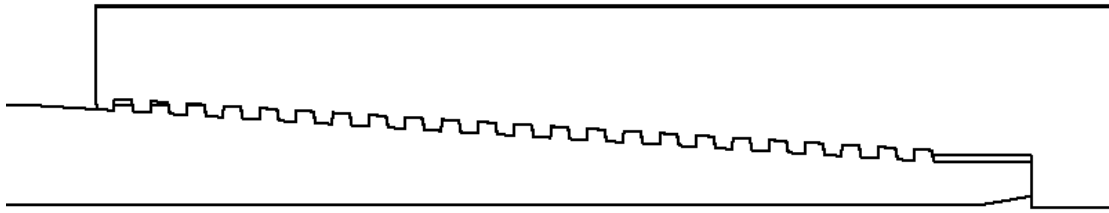


*Figure 8: Proprietary connection.*

Some of the proprietary connection with metal to metal sealing surface offer 100% connection efficiency in compression but tensional efficiency in the same range as conventional connections. This development has not gone unrecognized by the geothermal industry and connections of this type are considered as option for geothermal wells of the future including IDDP wells.

The widely used API BTC connection has proven to have certain limitations; it provides poor sealing in a high temperature setting and its tensional and compressional strength is a great deal lower than the pipe body strength. Therefore more advanced coupling options have attracted the attention of the geothermal industry.

## 2.5 Casing loads

A casing in a geothermal well is subjected to multiple loads during operation. The loads a casing has to bear are gravitational loads, thermal loads and pressure, both internal and external. The loads are categorized to axial loads that can be tensional- and compression load, burst load from internal pressure and collapse load from external pressure.

The load history begins when tripping into the hole and if residual stress from production is neglected the first load is tensional load during installation. The tensional load increases with length of casing string that causes the highest load to be on the uppermost part of the casing. The well is under normal circumstances full of water during installation. The buoyancy of the casing string can be used to reduce tensional loads during installation. This is done by not filling the casing string totally with fluid while running in hole [25].

When the casing string is in place, a common practice is to cement with inner string method, where a cement slurry is pumped down through a drill-pipe and up the annulus to surface. The difference between inner and annulus pressure is dependent on the density difference between the cement slurry and the fluid inside the casing [25]. When the cement slurry solidifies it bonds with the casing and the formation. The temperature at this point is the zero reference temperature since from now on the casing is fixed.

When a casing string has been cemented, drilling of next phase starts and next load is presented. During drilling fluid is circulated down the drill-pipe and up the annulus for cooling and to transport cuttings to the surface. During this phase the casing string is cooled down, circulated fluid is colder than the zero reference temperature and the concrete restrains contraction of the casing and axial tension builds up in the casing as it cools down [25].

When a geothermal well has been drilled, the wellhead master valve is closed. Initially, the wellhead is not under pressure but gas buildup inside the well might cause increased wellhead pressure and depression of the water level in the well. The increased pressure triggers a casing load.

The greatest loads the casing string experiences is when the well is in operation. The temperature of the geothermal fluid which is extracted is 200-500°C warmer than the zero reference temperature. The casing in a flowing well experiences high thermally induced stress that exceeds the elastic limit of the casing material.

The post yield load would not necessarily have to be a problem in a seamless world where the well is opened up once and stays open throughout its lifetime but in reality wells need to be closed occasionally and sometimes quenched with cold water for work-over. This cyclic thermal load can trigger casing failure and is an important factor to be considered for high temperature setting casing design.



## **2.6 Casing failure modes**

### **2.6.1 Failure mechanism**

A casing string is under immense load both static and quasi static during the lifetime of a well. A casing failure can be a result of unsatisfactory installation, poor cement job, insufficient design or other natural factors which can't be controlled.

In deep petroleum wells the main design factors for casing are fluid pressure and tensile load during installation but in a geothermal well the greatest loads are due to restrained thermal expansion.

### **2.6.2 Collapse**

Collapse of a casing can range in severity. A minor collapse might go unnoticed or reduce flow from the well while a total collapse can block flow and render the well inoperable.

The first potential collapse load appears when the cement slurry is pumped down a drill-pipe to the casing shoe and up the annulus. The collapse pressure is the difference between the internal and external pressure. The difference is a product of the density difference between the cement slurry in the annulus and the fluid inside the casing.

The collapse pressure;

$$P_{collapse} = P_{external} - P_{internal}$$

The maximum collapse pressure is at the bottom of each casing string. At surface the pressure outside the casing and inside is the same but the pressure difference increases gradually with depth if density difference is present. Buckling of a casing string from restrained thermal expansion can also cause casing collapse.

A casing failure is rarely a result of a single load factor but rather a combined load. Casing will buckle from intensive restrained thermal expansion but other factors can aid in the process. Boiling water, trapped in between casing strings (water

pocket) is amongst known contributors. Euler buckling can happen after the casing string is cemented. If there is enough un-cemented gap in the annulus the casing can act like a column and therefore Euler buckling can occur [26].

Buckling of a casing wall is a widely documented failure in geothermal wells. The primary cause of this buckling mode is restrained thermal expansion but other factors like, casing imperfections, reduced casing wall thickness and water pocket will encourage the process.

### **2.6.3 Burst**

The difference between the annulus pressure and the pressure inside the casing can't be allowed to exceed the burst resistance of the casing. Internal pressure produces tangential stress in the casing wall. If the tangential stress of the casing wall exceeds the ultimate strength of the material the casing will burst. The burst resistance of a casing is a function of material properties and thickness of the casing body.

### **2.6.4 Connection failure**

A casing string consists of 10-13 meter long pipes that are welded or connected with threaded couplings. Connection failures can be accounted for a large majority of all casing failures. Great tensional load causes the connection failures but fatigue from cyclic thermal load is also a well-known cause.

In deep geothermal wells the temperature differences are up to 2 times greater than in a conventional geothermal well and stress on couplings approaches the ultimate strength of the coupling in the first thermal cycle.

The severity of a connection failure can range from a small leakage to a pullout failure where the threads are stripped from the pin or the coupling and a gap is present. A break at the third thread from the outside of the coupling is a common coupling failure, at a weak point, where the thread profile reduces the casing wall thickness and the coupling is not fully supporting the pipe. [27]

Connection failures often go unrecognized since such failures do not always affect the well's performance but the consequences of a pullout failure can be severe if the failure occurs at a disadvantageous location in the well like near surface.

Casing thermal loads in a deep geothermal setting, where the production casing is in contact with supercritical fluids, is far greater than the loads studied in published research. The need for research in this field is therefore of extreme importance to support technical developments which will make extraction of naturally occurring supercritical fluids from the roots of geothermal systems an obtainable goal.

### **2.6.5 Fatigue failure**

Fatigue failure is a common failure in steel structures and mechanical parts. Fatigue failure is a failure from repeated loads which is not high enough to cause failure in a single application.

The most widely recognized forms of fatigue failure are high cycle failure (HCF) which happens when the stress is within the elastic limit of the material, and low cycle fatigue (LCF), which happens when the load causes plastic deformation in the material.

According to C. Teodoriu and G. Falcone [28] the fatigue behavior of a casing material subjected to large temperature variations during well's operational life can be classified as LCF.

Low cycle fatigue (LFC) is a failure mode that can be expected where stress is high enough for plastic deformation to happen in the material. The researches of C. Teodoriu and G. Falcone [28] indicate that the low cycle fatigue resistance of a buttress thread connection can be as low as 10 cycles under conventional geothermal conditions.

### **3 Methods**

#### **3.1 The research method**

The main objective of this analysis is to compare casing connection options and thread geometries available for high and extreme temperature geothermal well setting, in order to answer the research question; which type of casing connections examined, if any are best suited for extreme temperature setting and extraction of supercritical geothermal fluids from the bottom of a geothermal reservoir?

The selection of connection types and casing material for this research is to some extent based on papers published on the IDDP-1 and the IDDP-2 projects. The research is executed with the ANSYS workbench finite element analysis and simulation software which offers a combined thermal-structural option, well suited for the purpose of this research.

To investigate the performance and provide a ground for comparison, load cases are defined for the simulation. A casing string is under various loads during the lifetime of a well. The load cases defined are supposed to represent the conditions in a deep geothermal well which are most likely to challenge the capability of the casing string and the connections to the limits.

This research focuses primarily on impact of thermal expansion, other factors are neglected. Various assumptions and simplifications are made in order to reduce computation time. Excluded factors were carefully considered in order not to compromise the quality of the solution. The assumptions will be explained further when appropriate.

Both types of connections are subjected to identical loads and the initial and boundary conditions in the model are as alike as possible.

### **3.2 Finite element analysis (FEA)**

Finite element method (FEM) is a numerical method to obtain approximate solution to a system or a set of equations. The method can be applied to a variety of physical problems that can be described with governing differential equations.

Problems in engineering design can frequently be defined with differential equations, boundary conditions and initial conditions. The foundation for the equations are laws of nature and the differential equations describe a balance of e.g. mass, energy and force. Solution to the differential equation for a given system is a description of its behavior under given load, initial and boundary conditions [29].

Analytical solutions to differential equations which describe engineering problems are very rarely available. Analytical solutions mainly work for simple models but numerical methods need to be applied for complex problems.

The finite element method can be applied to problems with high complexity and unusual geometry and can be a valuable instrument where traditional methods lack effectiveness. It is in general not often possible to obtain an exact solution to a complex engineering problem and the common method used is to seek an approximate solution with numerical methods.

A threaded casing coupling under intensive thermal load is a definitive example of such a problem, multidimensional problem, non-linear material behavior and a complex geometry.

The steps towards a solution of computational model of an engineering problem can be described as follows; definition of the problem, mathematical modelling and simulation. The first step involves definition and idealization of the problem in terms of the quantities to be measured. The second step is the modelling step where the physical reality is defined by mathematical expressions, boundary and initial conditions. The third and final step towards a solution or approximation can be carried out with numerical methods [30].

FEM is as stated before, a numerical method to approximate a solution to a system. The method is carried out in three basic phases that each involves sub-phases. The first phase is the preprocessing process where the solution domain is discretized into elements, the infinite number of elements of the continuous body is divided into finite number of elements. The elements are connected with nodes and a shape function, a continuous function which describes the physical behavior of each element and the shape of the body between the nodes is established. The shape functions are continuous functions e.g. polynomials and represent the unknown quantity.

Each element has a certain shape which is defined by the user as well as the number of nodes that connect the elements. In a three dimensional unconstrained model each of the nodes has six degrees of freedom (DOF), three for linear displacement and three for rotation which means that each node is free to move in all directions and rotate around all axis of the Cartesian coordinate system. The nodes link the elements together and vice versa.

In the preprocessing phase all the elements are assembled to represent the entire problem, initial conditions, load and boundary conditions are applied. The second phase is a solution phase where a set of the shape functions are solved simultaneously for all nodes of the system with numerical methods. The unknown quantity can be e.g. temperature, pressure, displacement or voltage, depending on the nature of the system and the problem [29]. The third phase is the post processing phase where the results are interpreted and presented.

The finite element method offers both linear and non-linear approach. The linear method is sufficient when behavior of the body is linear. An example of a linear problem is a steel structure under stress that does not exceed the yielding point, as derived from Hooke's law the stress-strain relationship is linear within the elastic region of the material. When dealing with non-linearity, for example a steel structure which is stressed past the yielding point and is plastically deformed the problem can't be described with linear equations.

A linear finite element analysis of a structure stress or strain uses the stiffness of the part to compute response to applied load. A highly simplified matrix expression of the finite element solution for an elastic deformation of a body is;

$$\mathbf{F} = \mathbf{k} * \mathbf{d}$$

Where  $\mathbf{F}$  is a force matrix,  $\mathbf{k}$  is the stiffness matrix and  $\mathbf{d}$  is the displacement matrix. The stiffness matrix depends on the material properties and geometry. In a linear analysis the stiffness matrix is constant throughout the solution process and the behavior of the model is therefore linear.

If the problems requires a non-linear approach the process becomes more complex and constant stiffness is no longer existent. In order to simulate the non-linear response the stiffness matrix is altered throughout the solution process and the stiffness becomes a function of e.g. displacement and deformation of the body. The computation of a non-linear model is heavier than linear due to higher complexity of the equations describing the model.

### 3.2.1 Discrete system, general solution

According to O.C. Zienkiewicz and R.L. Taylor, [31] for any kind of discrete system e.g. finite element system, we can in general identify a set of discrete parameters, system parameters which represent the behavior of each element and the system as a whole, denoted  $\mathbf{a}_i$ . For each element a set of quantities  $\mathbf{q}_i^e$  can be computed in terms of the system parameters where in FEM system,  $\mathbf{e}$  is the element index and  $\mathbf{i}$  a nodal index. The relationship can be either linear or non-linear. The linear representation of the relationship can be expressed as;

$$\mathbf{q}_i^e = \mathbf{K}_{i_1}^e \mathbf{a}_1 + \mathbf{K}_{i_2}^e \mathbf{a}_2 + \dots + \mathbf{f}_i^e$$

Where  $\mathbf{f}$  represents nodal forces and  $\mathbf{K}$  is a constant e.g. a stiffness matrix if the problem is a structural problem.

The system equations are obtained by an addition where  $\mathbf{r}_i$  represents the system quantities.

$$\mathbf{r}_i = \sum_{e=1}^e \mathbf{q}_i^e$$

This yields a system of equations;

$$\mathbf{K}\mathbf{a} + \mathbf{f} = \mathbf{r}$$

Where

$$\mathbf{K}_{i,j} = \sum_{e=1}^m \mathbf{K}_{i,j}^e$$

And

$$\mathbf{f}_{i,j} = \sum_{e=1}^m \mathbf{f}_{i,j}^e$$

O.C. Zienkiewicz and R.L. Taylor, [31] also state that for the solution of a discrete problem like finite element problem, it is often convenient to establish a coordinate system for each element which is different from the coordinate system of the external forces applied and the displacements of the body are measured in. In a FEM a different coordinate system is established for each node of the discrete system. The coordinate system for individual nodes is called local coordinate system and the main coordinate system of the body is the global system. A transformation matrix is used to project between the local and global coordinate systems. The transformation matrix is here denoted  $\mathbf{L}$  and the properties in the local coordinate system are denoted with apostrophe. The local displacement  $\mathbf{a}'$  can be projected between the coordinate systems as described by O.C. Zienkiewicz and R.L. Taylor [31] by;

$$\mathbf{a}' = \mathbf{L}\mathbf{a}$$

And where the amount of the unknown quantity is the same in both systems;

$$\mathbf{q}^T \mathbf{a} = \mathbf{q}'^T \mathbf{a}'$$



If we insert for  $\mathbf{a}'$ , the local displacement, into equation;

$$\mathbf{q}^T \mathbf{a} = \mathbf{q}'^T \mathbf{L} \mathbf{a}$$

The equation can be simplified to;

$$\mathbf{q} = \mathbf{L}^T \mathbf{q}'$$

Which states that the total unknown quantity in the global coordinates is the transposed transformation matrix times the unknown quantity in the local coordinate system.

For each element we can state;

$$\mathbf{q}' = \mathbf{K}' \mathbf{a}'$$

Which states that the unknown quantity in the local coordinate system is the local properties e.g. stiffness matrix,  $\mathbf{K}'$  times the local displacement.

Which can be rewritten with insertion as;

$$\mathbf{q} = \mathbf{L}^T \mathbf{K}' \mathbf{L} \mathbf{a}$$

Which states that the unknown quantity in the global coordinate system is transposed transformation matrix times local properties, e.g. stiffness matrix times the transformation matrix times the displacement in the global coordination system.

$$\mathbf{K} = \mathbf{L}^T \mathbf{K}' \mathbf{L}$$

When the discrete system has been described by the set of equations, the unknown quantity can be approximated by solving the system of equation simultaneously with numerical methods, e.g. Newton-Raphson.

### 3.3 Modeling of the connection

The models were built in Inventor, a 3D CAD program, and analyzed with ANSYS Workbench 15 from ANSYS, Inc. (ANSYS), a finite element simulation software which supports coupled thermal-structural analysis of complex geometries. Though the ANSYS program is able to handle complex geometries the model has to be simplified in order to reduce computation time. The model is simple enough to allow efficient computation but takes into account all essential features of the problem, the model is as simple as possible but not too simple.

A casing coupling is under various loads during its operational lifetime but the load considered in this study is restricted thermal expansion. A well casing and its connection are symmetric around the length axis as well as the loads prompted by the constraint thermal expansion examined in this study. It is therefore possible to examine a section of the connection rather than the full pipe and coupling. The ANSYS software offers constraints which allow symmetrical objects to be sectioned and a section can be analyzed. The results for the sectioned model then represents the model as a whole if boundary conditions are properly defined.

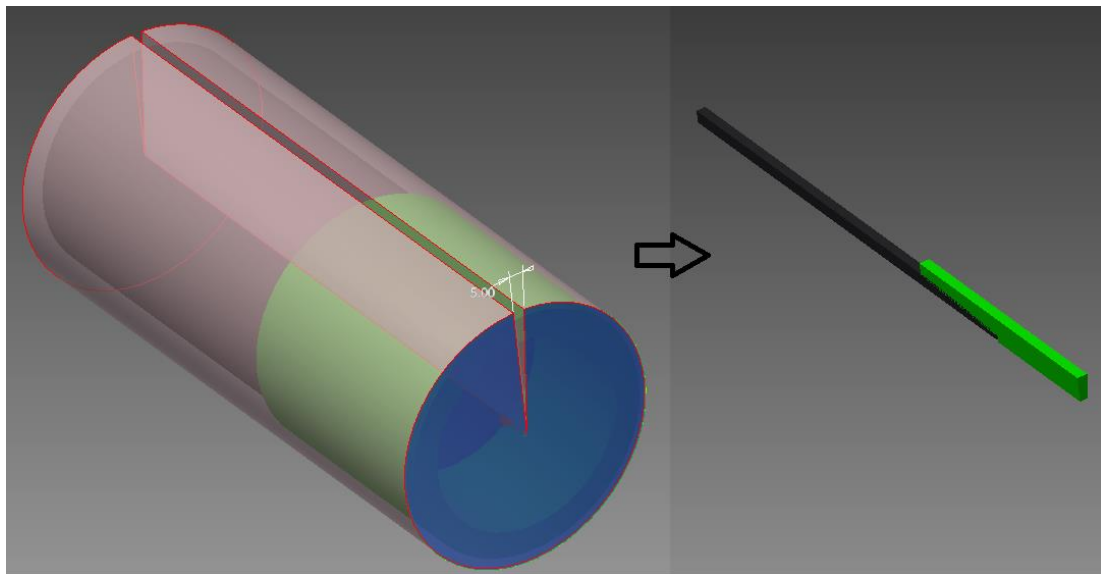


*Figure 9: The model and section.*

### 3.3.1 The material

The material model is specified according to the standard API-5CT, European pressure vessel standards and articles on material properties at elevated temperatures [32] [33] [34]. The most essential material properties included in this model are yield strength, coefficient of thermal expansion, elasticity and Poisson's ratio. Properties of steel in general change with temperature. The most important factors concerning this experiment are changes in yield strength and elasticity with elevated temperature.

The API-5CT standard specifies grades for casing steel. The grades specify material requirements but are not a material standard. This means that various types of material can be in the same grade since the grades in general specify minimum properties.

The literature is not consistent regarding the thermal properties of casing material. This might be related to the width of the material grades specified in the casing material standards commonly used. This research therefore takes a conservative approach regarding material properties in order not to overestimate the quality and effectiveness of a casing connection.

The material model inputs are displayed in the Table 1. The ANSYS software interpolates to determine material properties between and outside the input points.

T(°C)	K55, Yield Strength (MPa)	L80, Yield strength (MPa)	Modulus of elasticity (Pa)	Poisson's ratio
22	380	550	2.1E+11	0.3
100	285	412		0.3
150	270	390		0.3
200	258	374	2E+11	0.3
250	243	352		0.3
300	228	330	1.9E+11	0.3

*Table 1, Material properties*

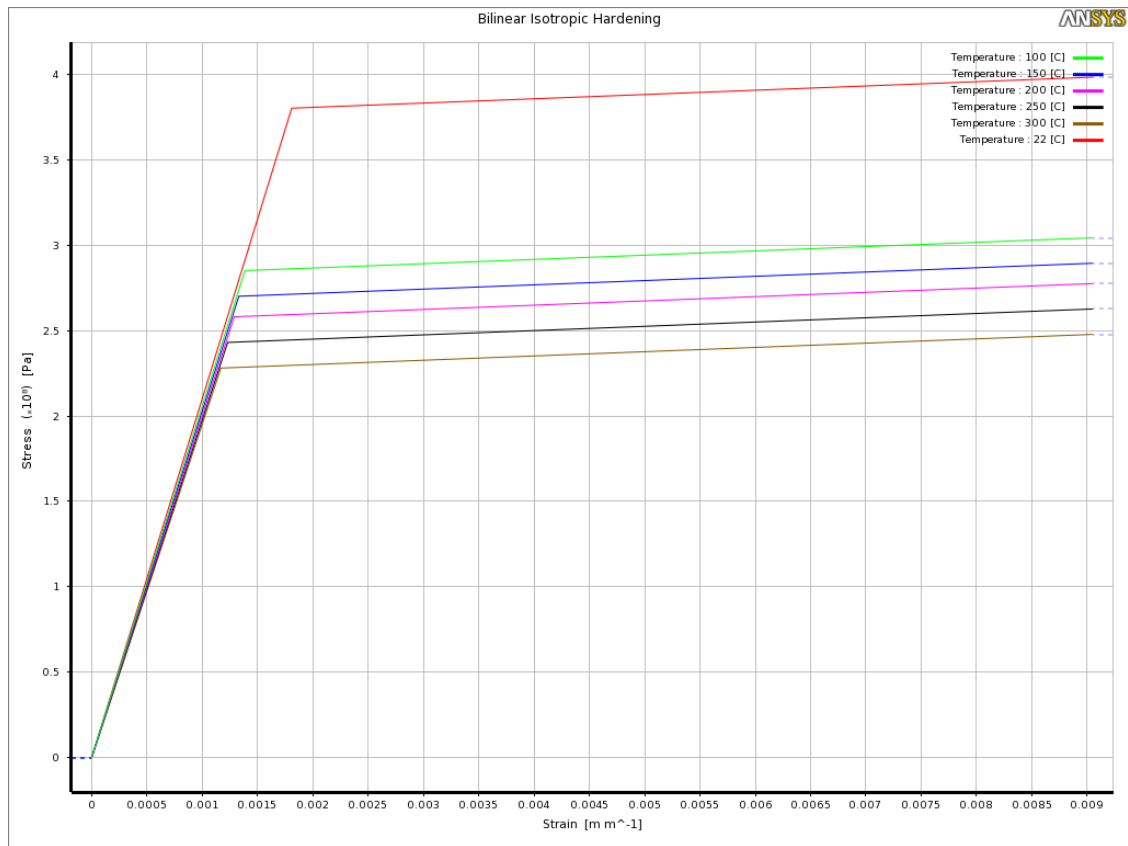


Figure 10: Assumed properties of K55 casing material

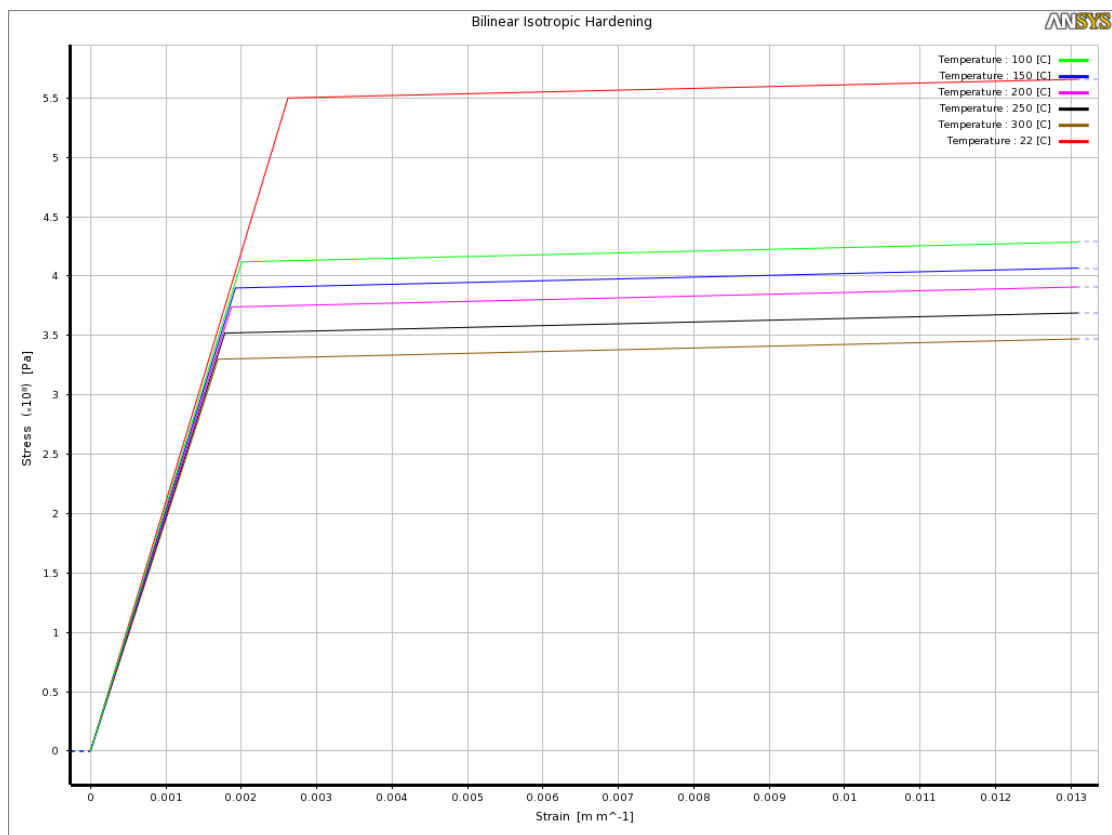


Figure 11: Assumed properties of L80 casing material.

The yield strength values used were derived from European pressure vessel standard. The values used are from the standards design criteria for steel at elevated temperature.

Standard Association of New Zealand (NZS) published Code of practice for deep geothermal wells (CPDW) in 1991 and a revised version in 2015. The NZS standard has been used worldwide by the geothermal industry as a foundation for design and practice. The NZS CPDW standard from 1991 includes a chapter on casing design and thermal load. Factors for reduced yield strength and changes in modulus of elasticity are published but it is noted in a disclaimer that sufficient published test data is not available for the casing grades involved. The NZS CPDW approach to this matter is less conservative than the material model used in this study but not by far, the standard suggests that for every 100°C increase in temperature, the yield strength is reduced by 5% [35].

The NZS CPDW can't go unmentioned as it is and has been an important document widely referred to by the industry and scientists. The information on casing material properties at elevated temperature in the standard are however published with disclaimer and therefore not used directly in this study.

### **3.3.2 Model and meshing**

The model is a 5° section of the pipe and coupling. The length of the pipe is 500 mm and the coupling is in standard length, 270 mm. In this case a single connection is modeled and any details outside the boundaries of the threads are neglected. Threads are modeled according to the API specifications.

The metal to metal seal premium or proprietary connection model shaped by the author represents the concept but not a specific brand or API standard connection. Each producer has a unique implementation of the metal to metal seal but the concept is the same.

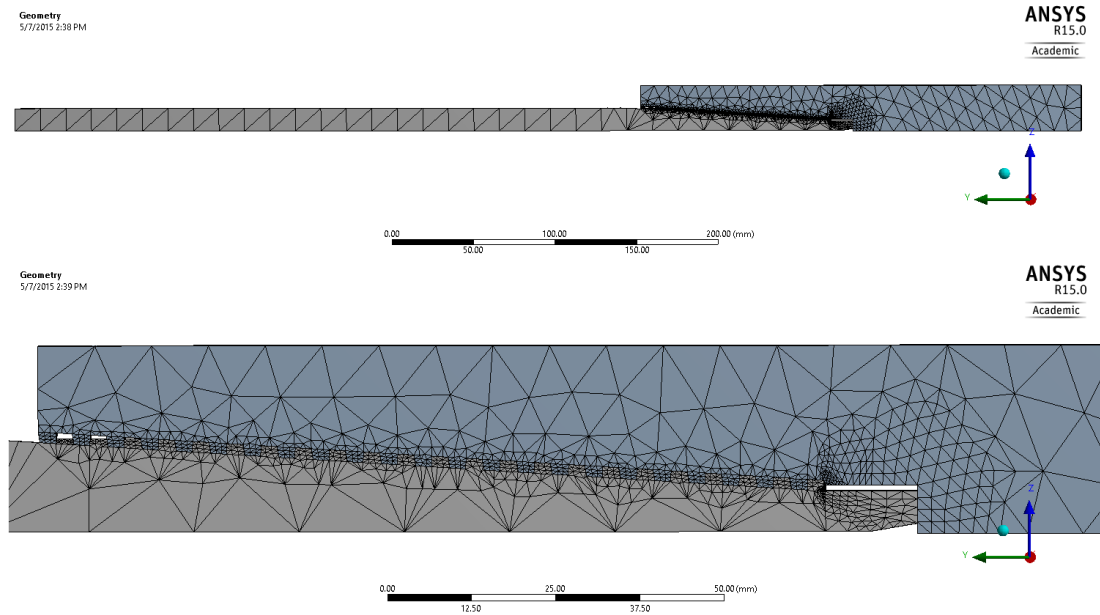


*Figure 12: The model mesh, proprietary connection.*

In Figure 12, the proprietary connection and meshing are displayed. The meshing is automatic but refinement is inserted on critical sectors to improve the accuracy of the solution. The meshing is identical in all models and the constraints are the same to provide basis for comparison. The contacts are frictionless so the bodies can slide without obstruction axially and radially. The boundary conditions are further explained later in the text.

### **3.3.3 ANSYS model setup and constraints**

The body studied in ANSYS is a 5° section of the pipe with coupling. In order to ensure the sanity of the solution, proper boundary conditions have to be defined. The movement and expansion of the section has to be constrained with boundary conditions applied accordingly to ensure expansion and movement of the section represent the pipe and coupling as a whole. The thermal load is applied gradually and the temperature increase of the material is homogenous.

Regarding the structural constraints, the sides of the section are supported with a frictionless support which allows radial displacement but restricts tangential

movement. The inside of the pipe and coupling are supported with a cylindrical support which restricts radial and tangential displacement, on the outside only tangential displacement is restricted. All parts of the body are free to expand axially but both ends are fixed.

A firmly cemented casing string is well supported. The most severe load points occur where the casing string is not firmly cemented. Un-cemented or poorly cemented sections are inevitable in a very deep well. This case study assumes that the joint is not radially supported by cement but fixed on both ends.

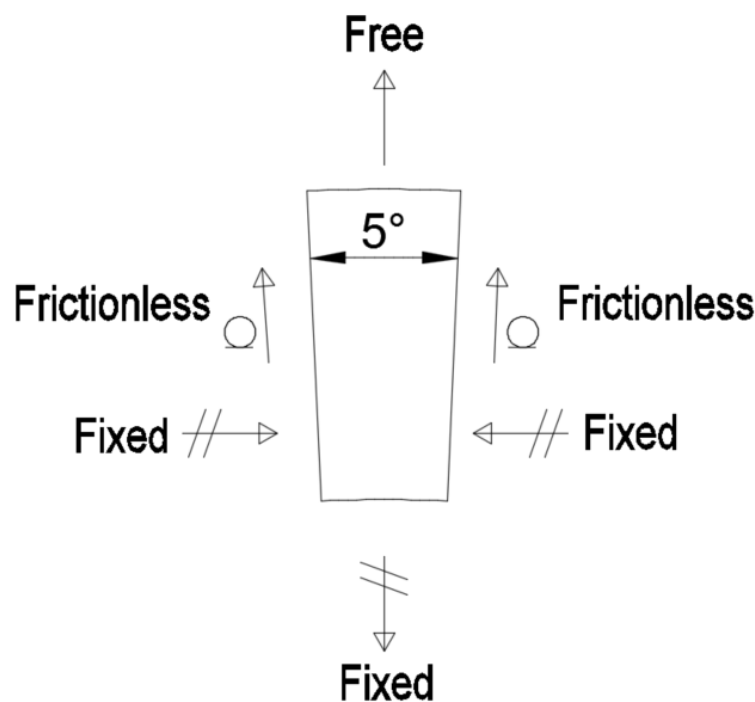
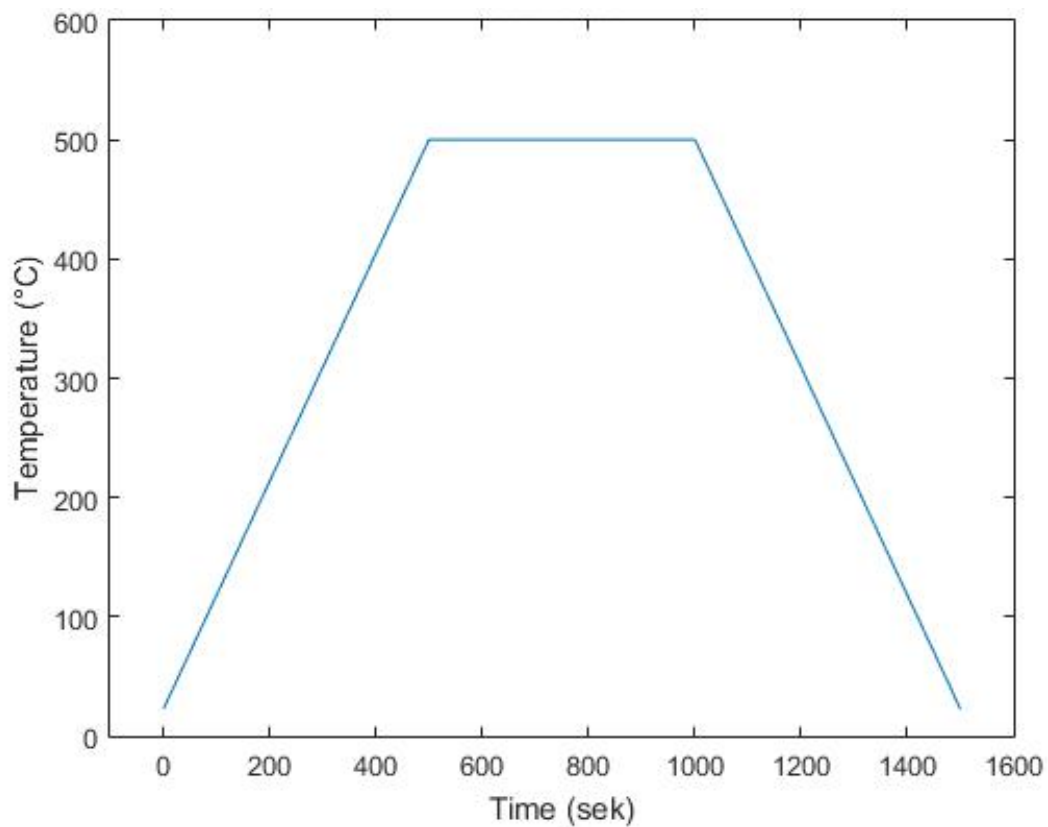


Figure 13: The boundary conditions.

### 3.3.4 Load case 1

The first load case examined which can be seen in Figure 14, is a slow heat up followed by a period of constant temperature and then ultimately the model is cooled back down to the initial temperature. Load is applied gradually, slow enough to ensure uniform heating. This scenario is invented to represent the initial warm up of the well followed by the first quenching. Time dependent properties are not included in the material model therefore the “hold” period is long enough to ensure that all the material has been heated up to the maximum

temperature but no longer. Here the material is heated to 500°C which is near the highest fluid temperature expected near a magmatic body.



*Figure 14: Thermal load, case 1.*

### **3.3.5 Load case 2**

The second load case, displayed in Figure 15 is a cyclic load case. The “well” is heated up to 400°C four times. The load is altered slowly like in the first step to ensure uniform heating and cooling of the casing body. The heat up and cool down happen at same pace as the first load and the maximum temperature “hold” period is long enough to ensure that all the material reaches the maximum temperature. This load case simulates a case where the well has to be opened and closed multiple times or heated up and quenched repeatedly.



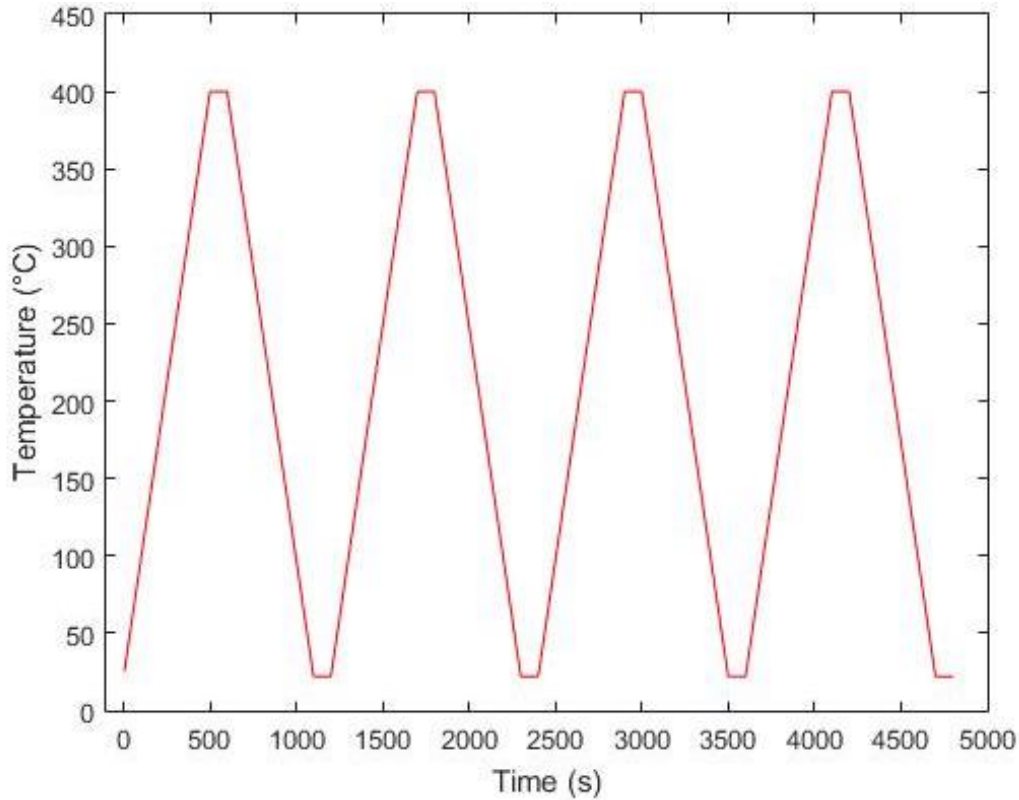


Figure 15: Thermal load, case 2.

### 3.3.6 Load case 3

The third load case simulates a scenario where the casing string is cemented in tension. The purpose of this part of the experiment is to estimate if something is gained from applying tensional load on the casing string when the cement slurry hardens. According to industry experts, the cement slurry solidifies partially during the cementing operation of a long casing string and it is possible to apply tension on the casing string while cementing from bottom up [27]. This means that when the well heats up, initially the thermal expansion of the material releases the tensional load and theoretically the casing string goes into compression at higher temperature than if the cement hardens around the casing in neutral stress state. The compressional forces from restrained thermal expansion are also expected to be lesser than in a casing string cemented in little or no tension.

## **4 Results**

The results are presented with data and figures from ANSYS workbench. Matlab is used to handle numerical data and construct plots.

In the strain figures the deep blue color represents the elastically deformed material but lighter shades of blue, green and red represent plastic deformation. To begin with the results from the analysis of a conventional API BTC connection are presented and then the results for the proprietary connection. The load cases are presented separately.

### **4.1 Results for connection type 1, grade K55**

#### **4.1.1 Load case 1, API BTC, K55**

From Figure 16 to Figure 20, the stress and plastic strain in the connection throughout load case 1 is displayed. Each figure consists of two subfigures. In the upper sub figure the von-Mises stress is displayed and in the lower sub figure the plastic strain. The deep blue color in the lower sub-figure indicates no deformation or elastic deformation and lighter shades indicate that plastic deformation is present.



Figure 16: Load 1, API BTC  $t=0$ .

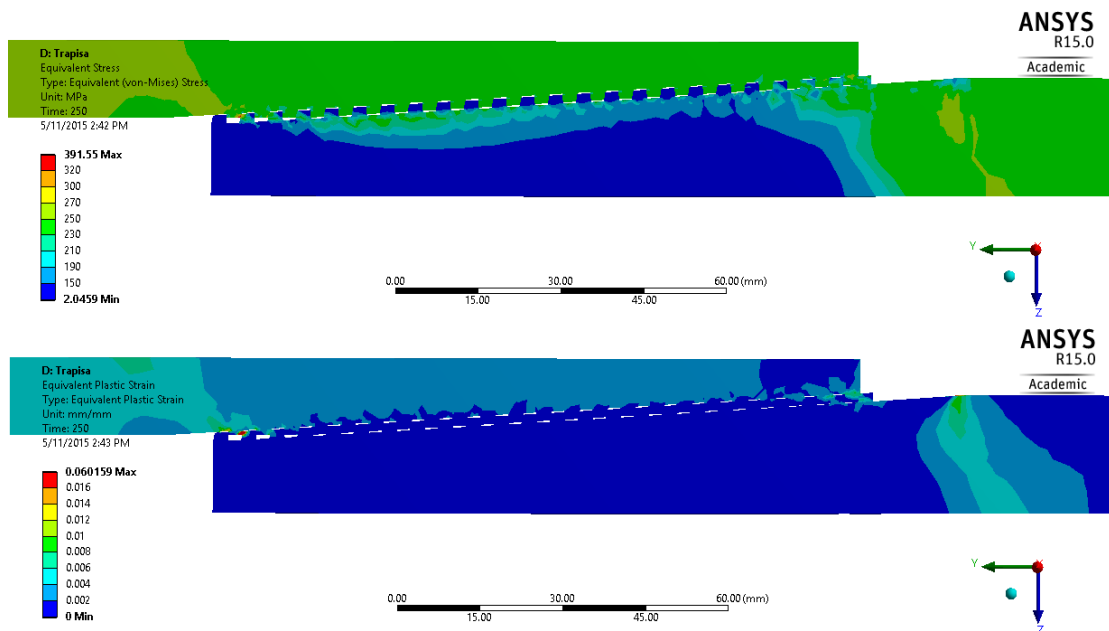


Figure 17: Load 1, API BTC  $t=250$ .

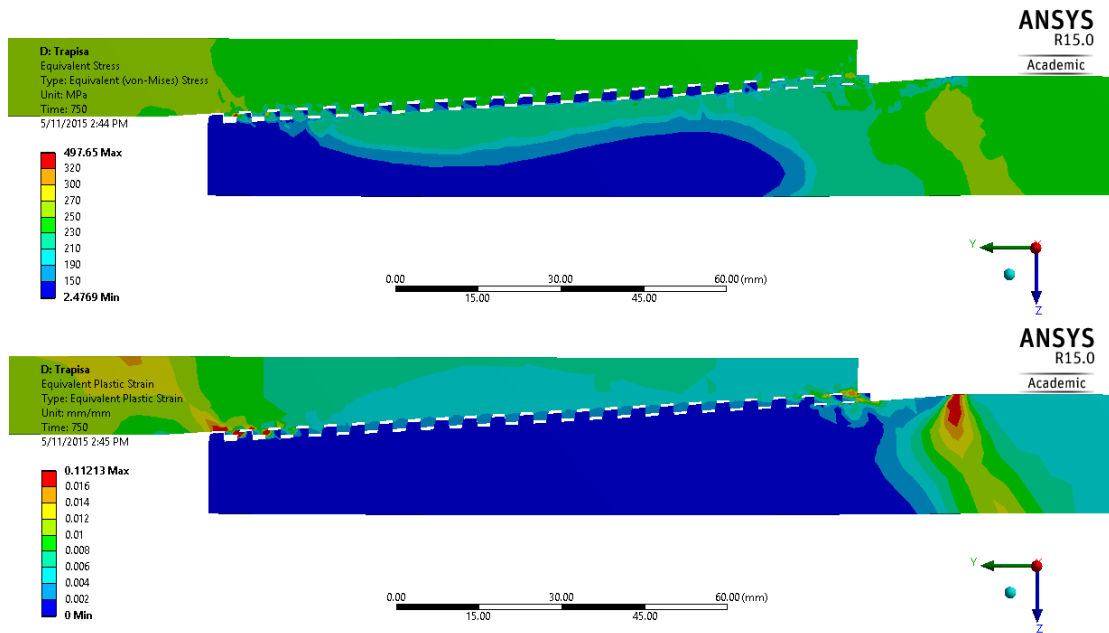


Figure 18: Load 1, API BTC  $t=750$ .

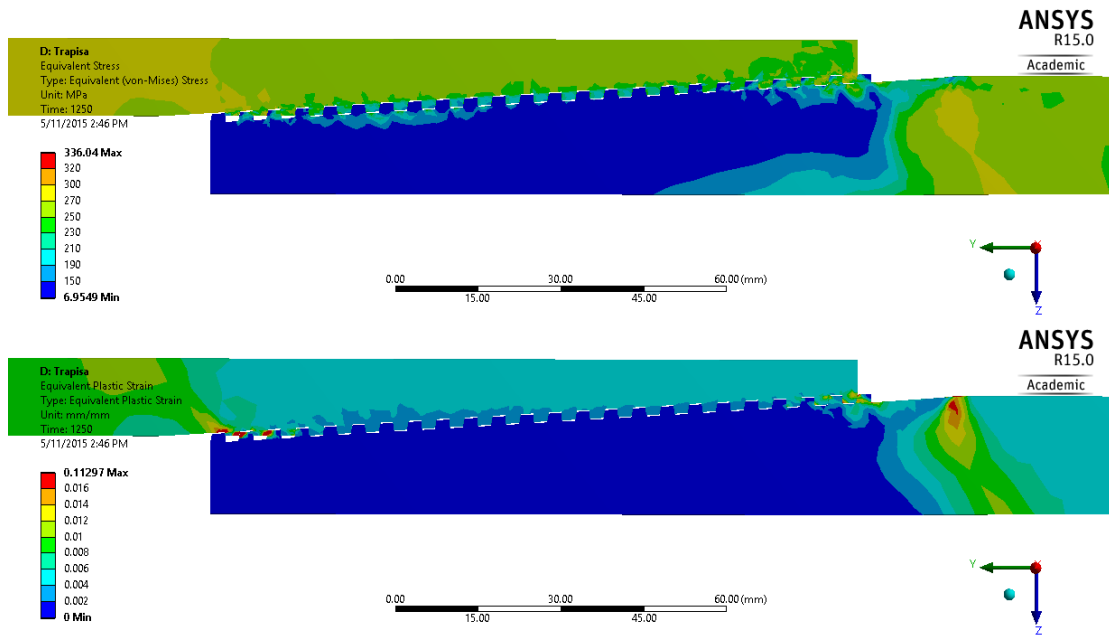


Figure 19: Load 1, API BTC  $t=1250$ .

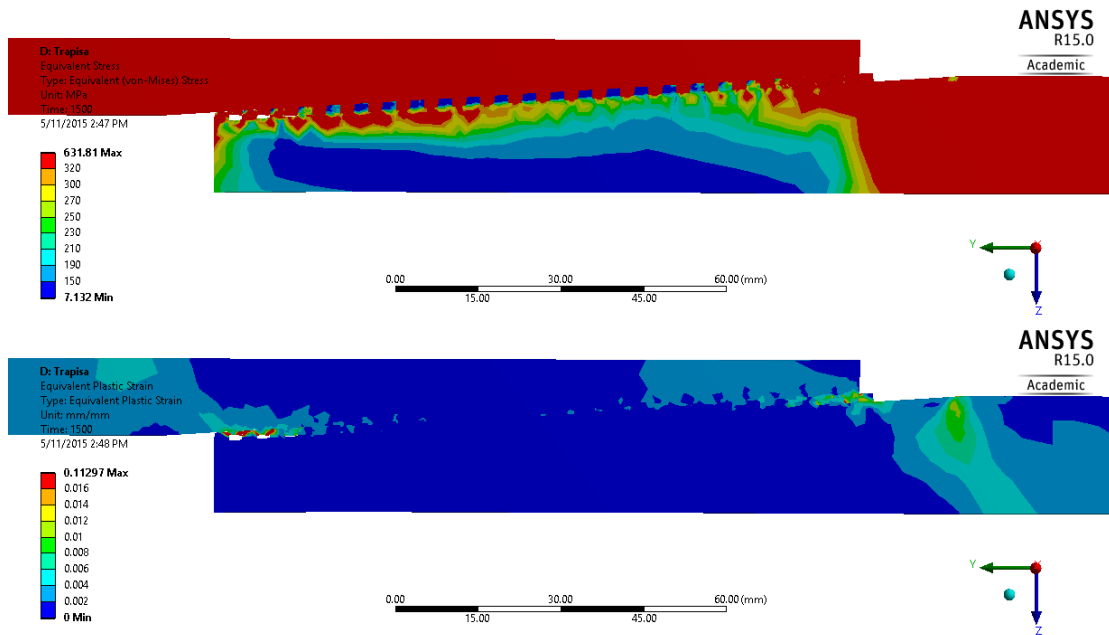


Figure 20: Load 1, API BTC  $t=1500$ .

Figure 16 to Figure 20 clearly present how heavily plastically deformed the casing coupling is throughout the load cycle both when it is compressed by the thermal expansion and when it is cooled back down to initial temperature.

Figure 21 presents the reactive axial force and temperature for load case 1. The casing string is plastically deformed from around 150°C and to the maximum temperature. The tensional forces are greater than the compressional forces since the yield strength decreases with increased temperature.

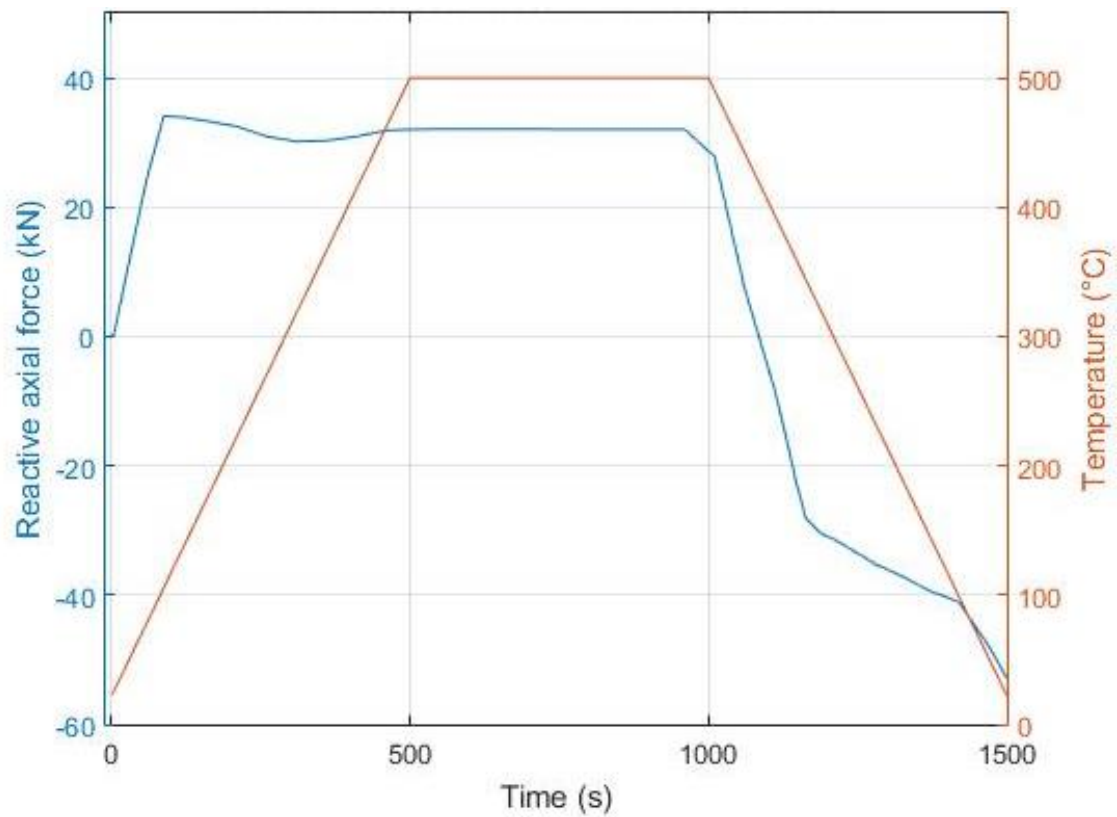


Figure 21: API BTC, K55, reactive axial force, load 1.

Figure 22 displays the elastic strain and deformation of the pipe end and coupling throughout the load cycle. The first subfigure presents the initial condition and the second one is where full load has been applied. The third sub-figure is at  $t=1250$  s and the last one at the end of the load step, at  $t=1500$  s. It is clearly presented how the coupling is forced outwards and the pipe end is forced to contract.

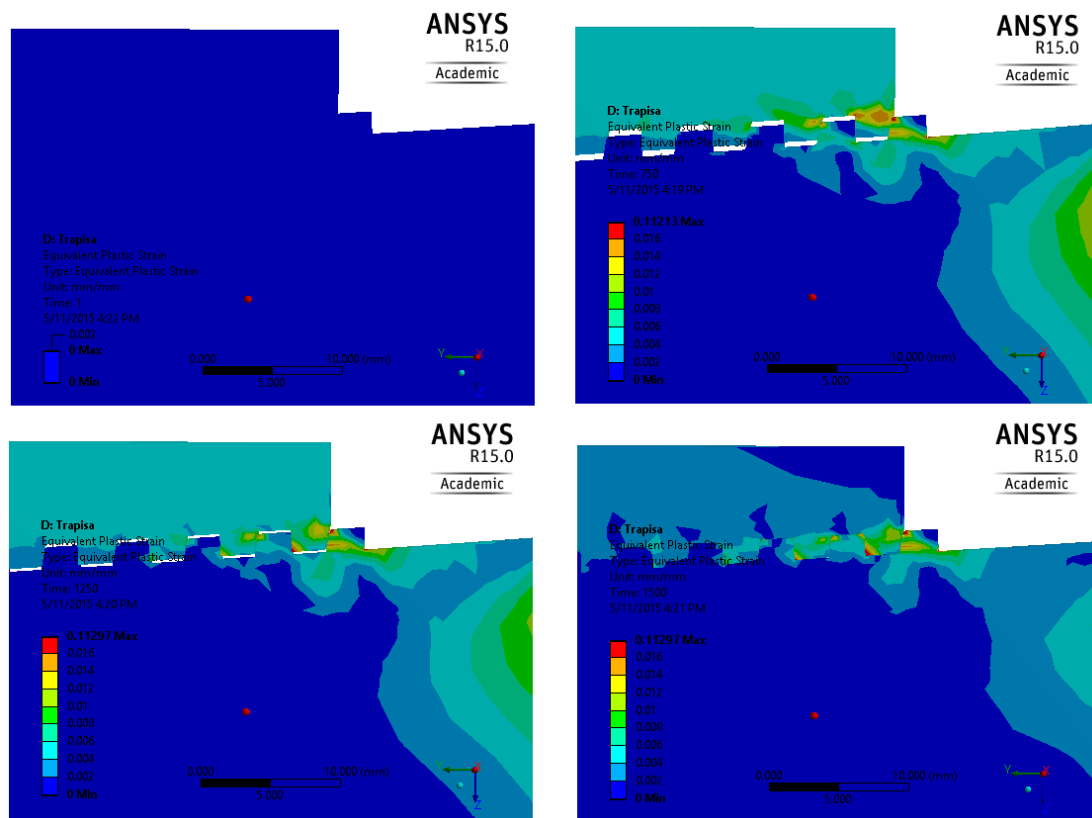


Figure 22: API BTC, pipe end deformation, load 1.

#### 4.1.2 Load case 2, API BTC, K55

The reactive axial force for the cyclic load case are presented in Figure 23. The pipe body is heavily plastically deformed both during heat up and discharge and when the well is cooled back down to 22°C. The axial forces increase between load steps due to hardening of the material.

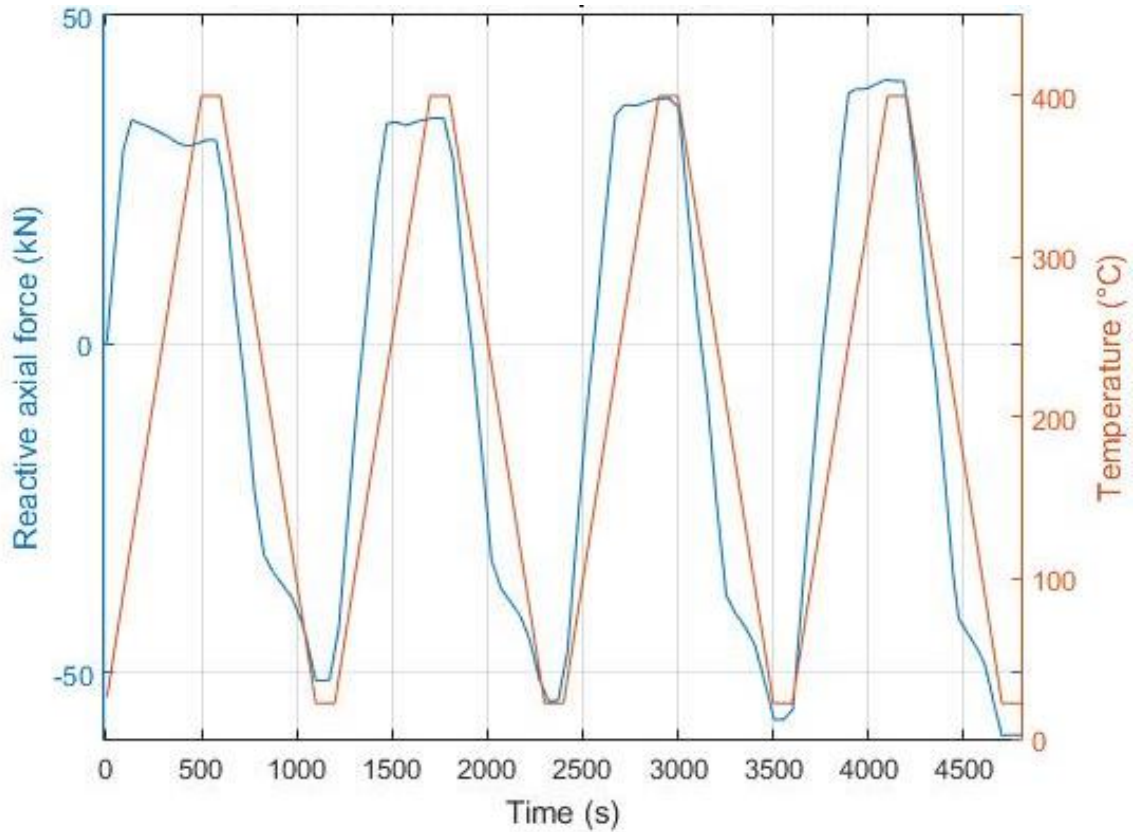


Figure 23: API BTC, K55, reactive axial force load 2.



## 4.2 Results for connection type 2 (Proprietary connection), grade K55

### 4.2.1 Load case 1, premium connection, K55

From Figure 24 to Figure 28 the von Mises stress and elastic strain at five points in load cycle one are displayed. Figure 24 shows the stress less state in the beginning, Figure 26 is half way through the cycle where the compressional load is at maximum. Figure 28 presents the state of the body at the end of the load cycle where the material has been cooled back down to initial temperature. The most interesting aspects are the separation of the threads, the coupling slides up away from the bottom of the threads as the body heats up. Another interesting detail which is displayed clearly is that initially the sealing surface gap is none but after one load cycle the separation is clearly visible. The colors are altered to follow the decrease in yield strength with higher temperature. In the lower sub-figure, the strain figure, the blue color indicates no deformation or elastic deformation while other colors indicate plastic deformation.

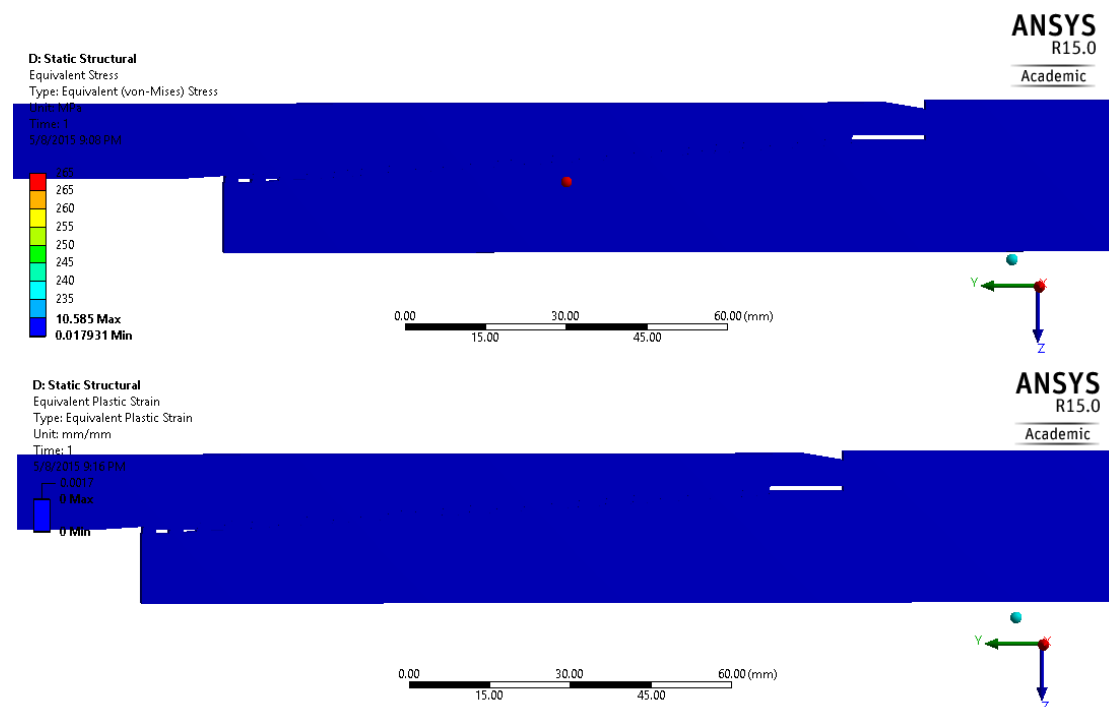


Figure 24: Load 1, Proprietary connection  $t=0$ .

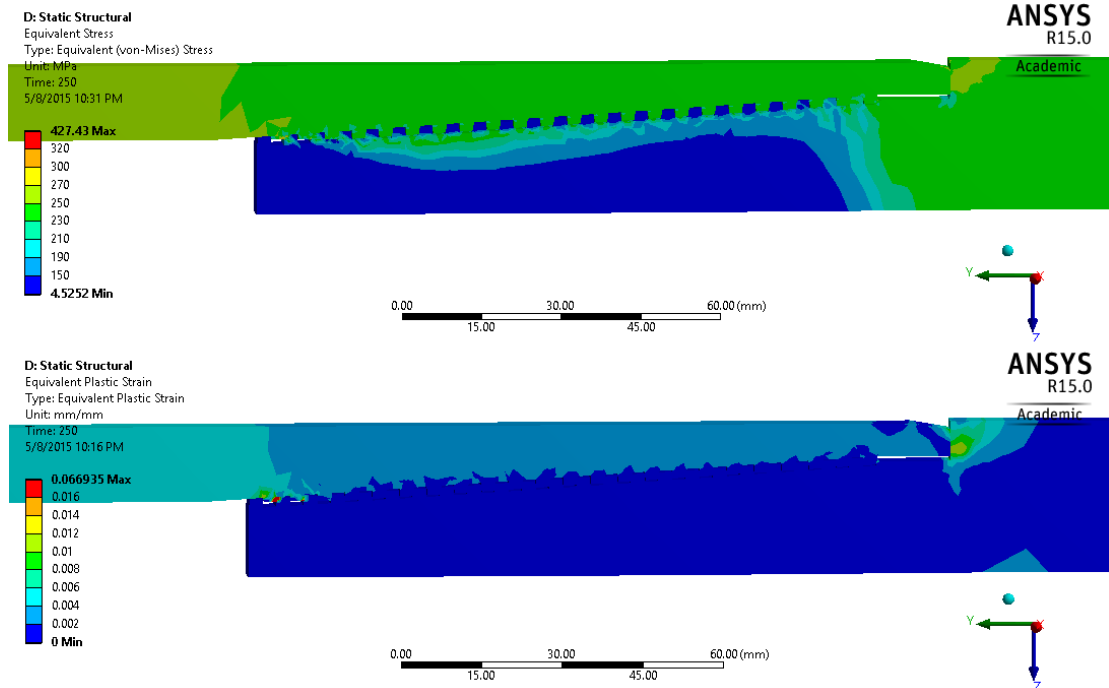


Figure 25: Load 1, Proprietary connection  $t=250$ .

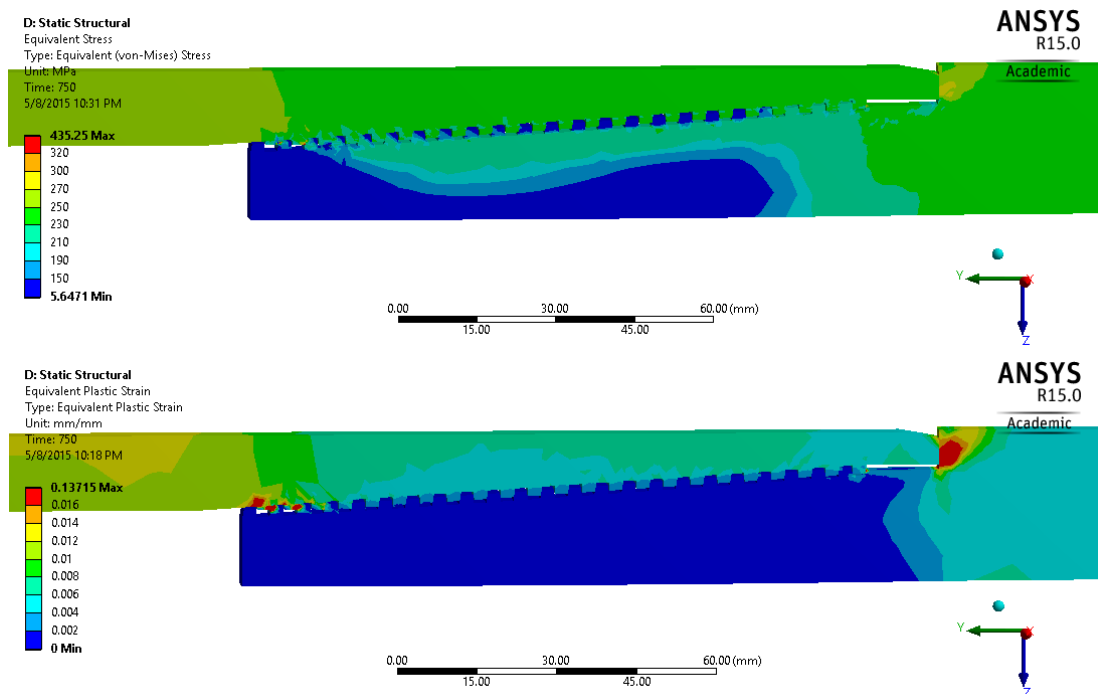


Figure 26: Load 1, Proprietary connection  $t=750$ .

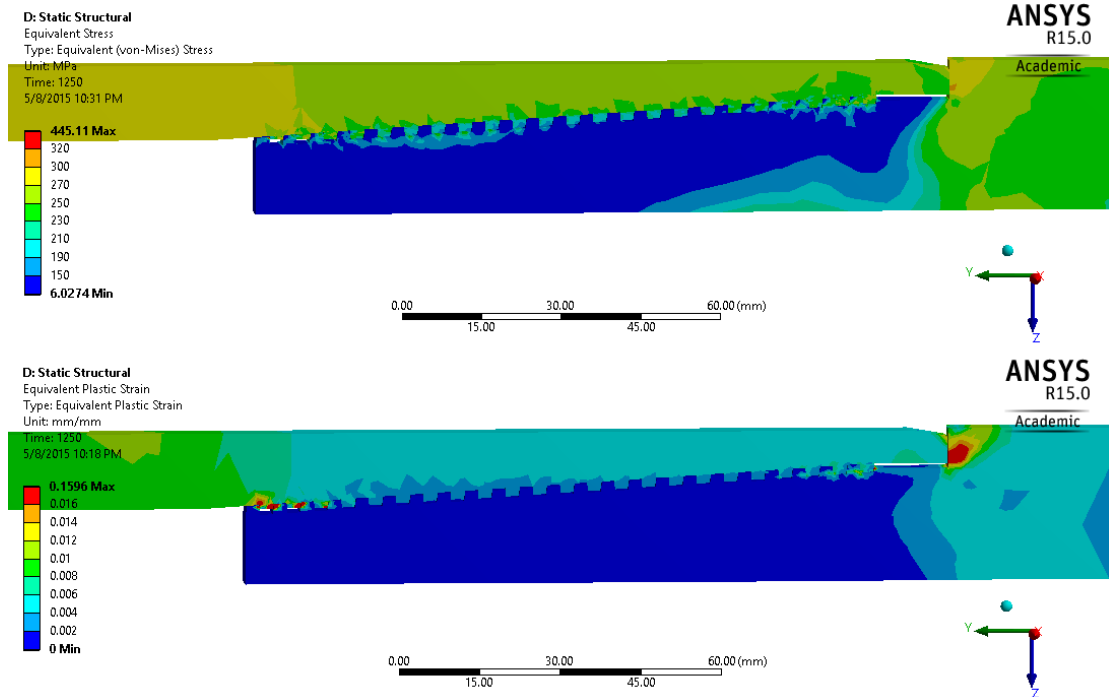


Figure 27: Load 1, Proprietary connection  $t=1250$ .

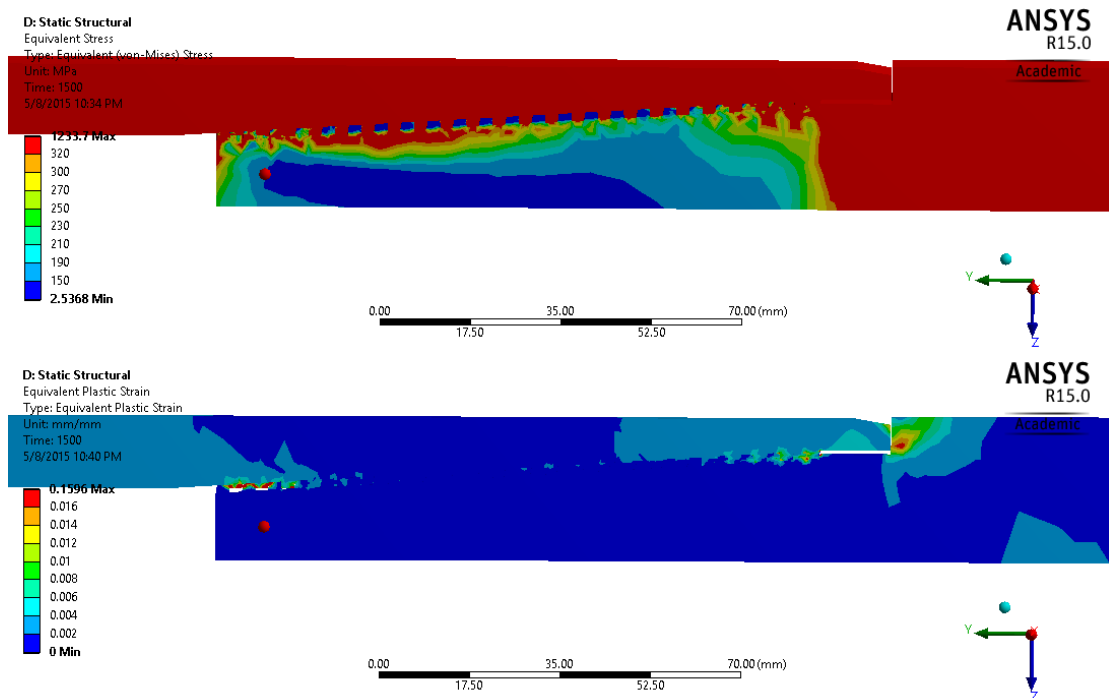


Figure 28: Load 1, Proprietary connection  $t=1500$ .

Figure 29 to Figure 33 focus on the sealing surface and the end threads near the metal to metal seal. In the beginning the sealing surface on the pipe and connection are in contact and the inside of the well is sealed from the outside. As the load increases the contact pressure decreases and plastic deformation occurs at the pipe and the connection. As the material is cooled down the material contracts and the sealing surfaces separate.

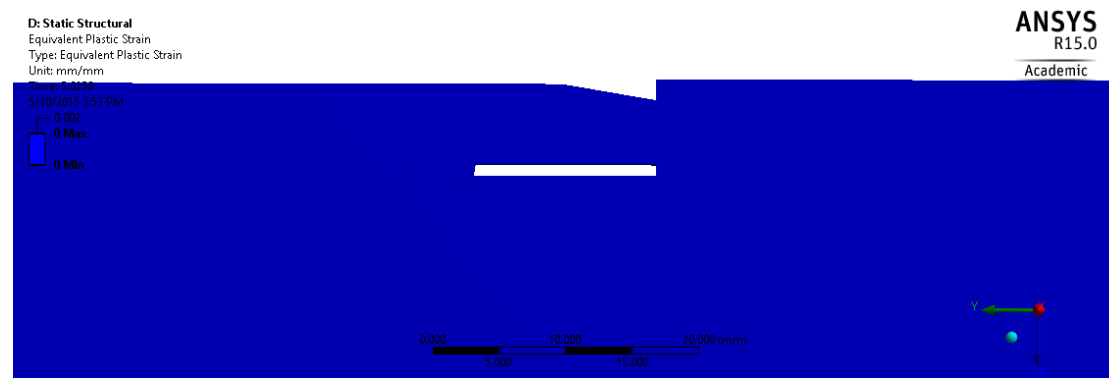


Figure 29: Load 1, Proprietary connection sealing surface  $t=0$ .

In Figure 29, before the thermal load is introduced the material is stress free and the sealing surfaces are in contact.

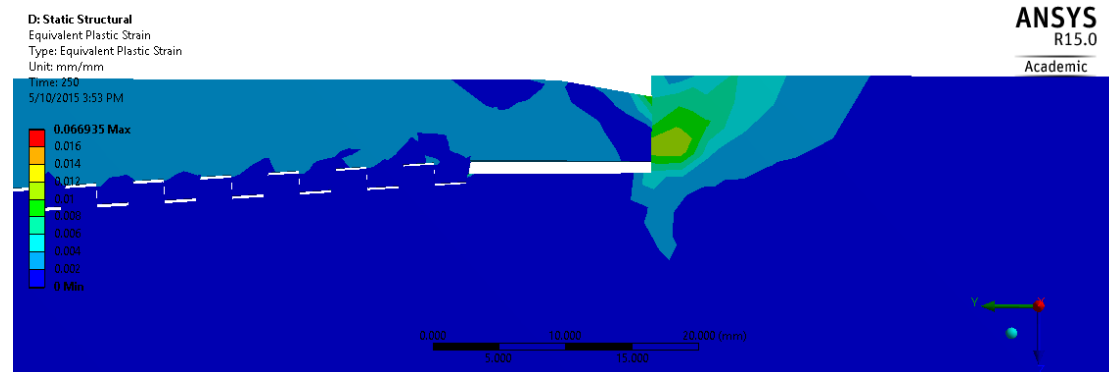


Figure 30: Load 1, Proprietary connection sealing surface  $t=250$ .

In Figure 30 the temperature is 250°C, plastic deformation is already evident and the pipe is forced to contract and the coupling to expand as can be perceived by the thread separation.

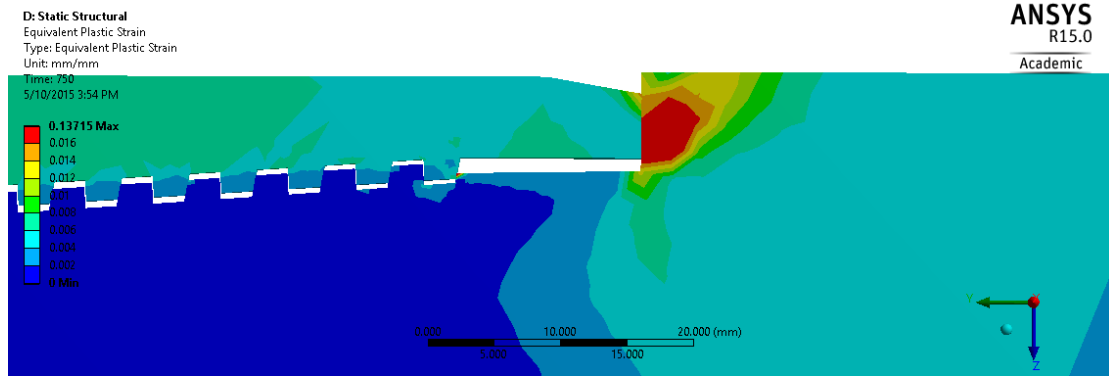


Figure 31: Load 1, Proprietary connection sealing surface  $t=750$ .

In Figure 31 the thermal load is at maximum level. The pipe body is plastically deformed and so are parts of the coupling. The heavy plastic deformation at the connection and near the sealing surface is both due to compressional forces and also bending forces as the coupling is forced outside away from the pipe body.

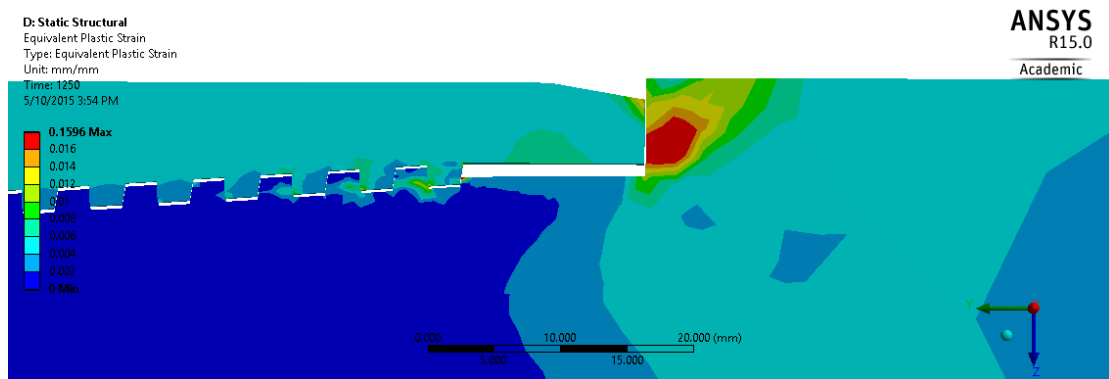
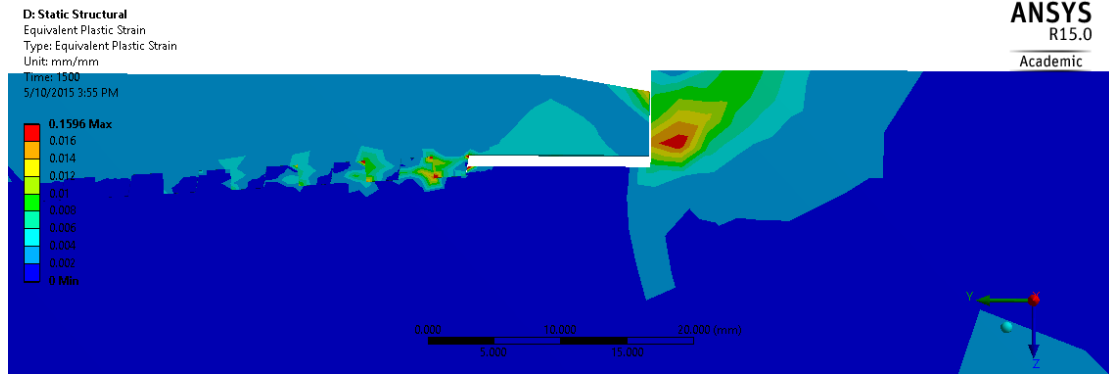


Figure 32: Load 1, Proprietary connection sealing surface  $t=1250$ .

In Figure 32 the well is being cooled down and is at 250°C. The casing is already in enough tension to cause plastic deformation and the seal is no longer tight. The plastic deformation near the sealing surface is due to bending which can clearly be seen by thread separation.



*Figure 33: Load 1, Proprietary connection sealing surface  $t=1500$ .*

In the last figure of the series, Figure 33 the material has been cooled down to the initial temperature. The tensional forces in axial direction cause yielding in the pipe and coupling body and the first 5 threads are heavily plastically deformed. The sealing surfaces are no longer in contact and the coupling is heavily plastically deformed from contraction forces.

Figure 34 displays reactive forces in axial direction and the temperature for comparison.

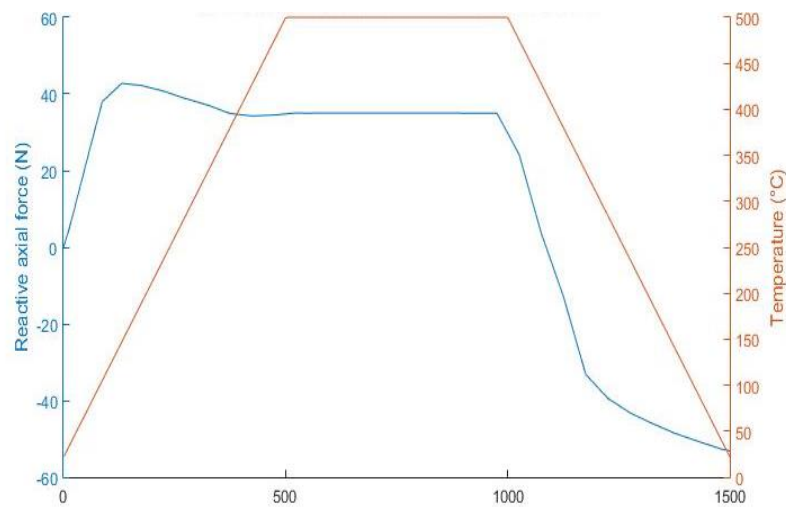


Figure 34: Load 1, Proprietary connection, K55, reactive axial force.

Figure 35 presents the contact pressure on the metal to metal sealing surface over the load cycle and temperature.

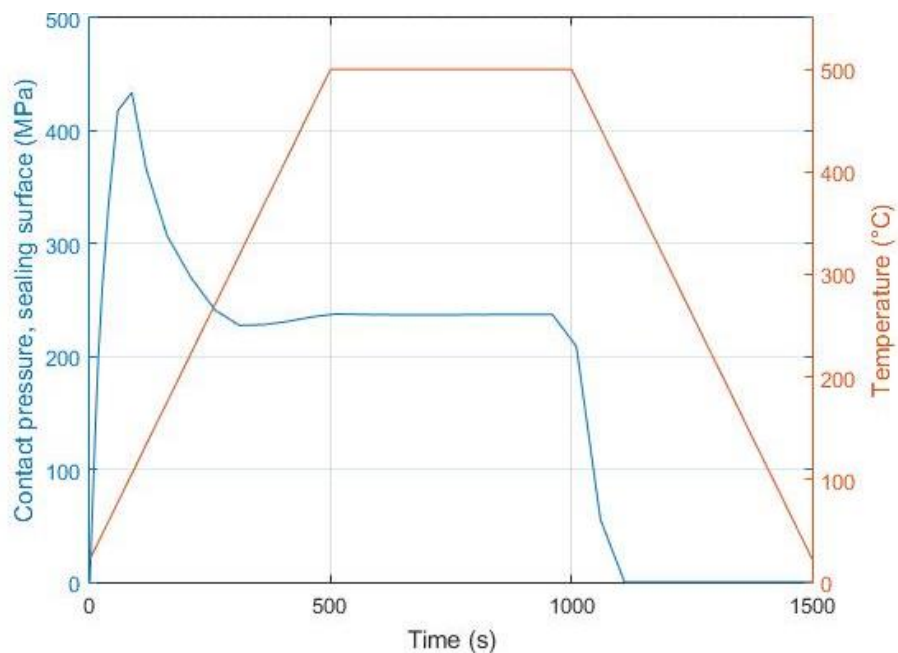


Figure 35: Load 1, Proprietary connection, K55, sealing surface contact pressure.

The contact pressure in Figure 35 decreases with decreased yield strength. It is clear that the contact pressure decreases fast as the body cools down from the maximum temperature and the surfaces are separated soon after cooling from maximum temperature.

#### 4.2.2 Load case 2, premium connection, K55

The stress and strain distribution in load case 2 is identical to load case 1 though stress and strain levels are different between load cycles.

In this chapter important results that highlight the effects of cyclic thermal load are highlighted.

Figure 36 displays the axial forces which increase in every load cycle do to hardening of the material.

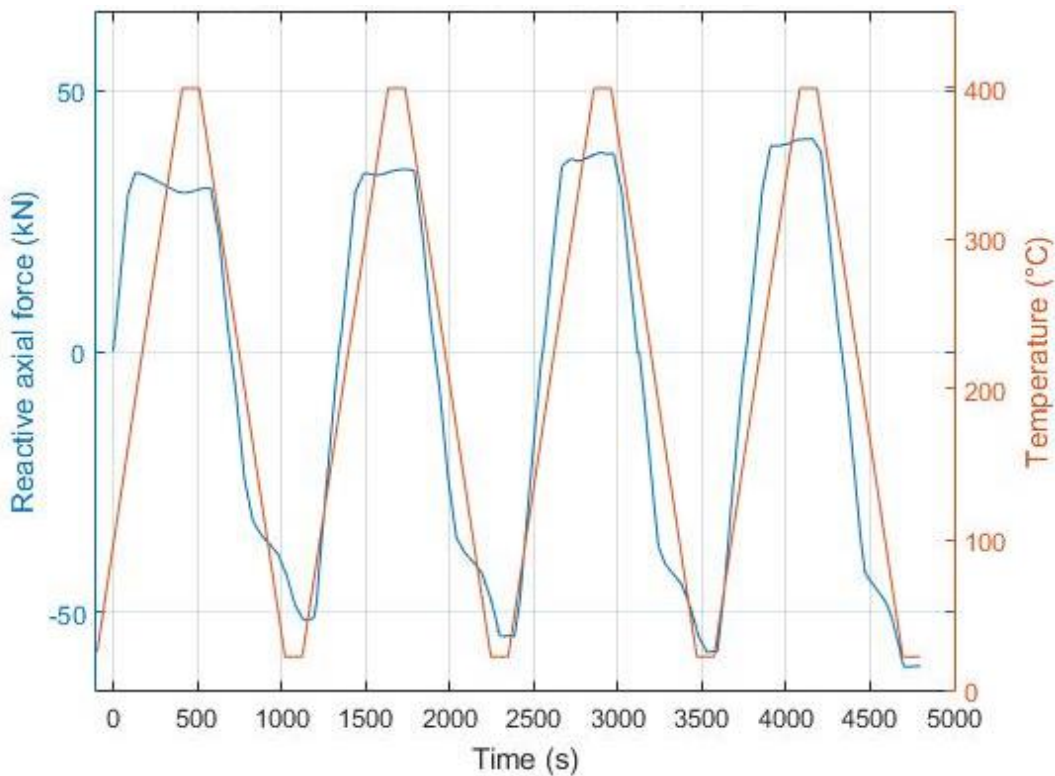


Figure 36: Load 2, Proprietary connection, K55, reactive axial force.

Figure 37 and Figure 38 display the status on the sealing surface. Figure 37 indicates contact pressure and Figure 38 the gap between the sealing surface on the pipe and the coupling.

From Figure 37 and Figure 38 it can be concluded that the metal to metal seal is vulnerable to plastic deformation due to axial thermal expansion. The separation of sealing surfaces happens very quickly after cooling from maximum temperature begins and happens earlier in every subsequent load cycle.



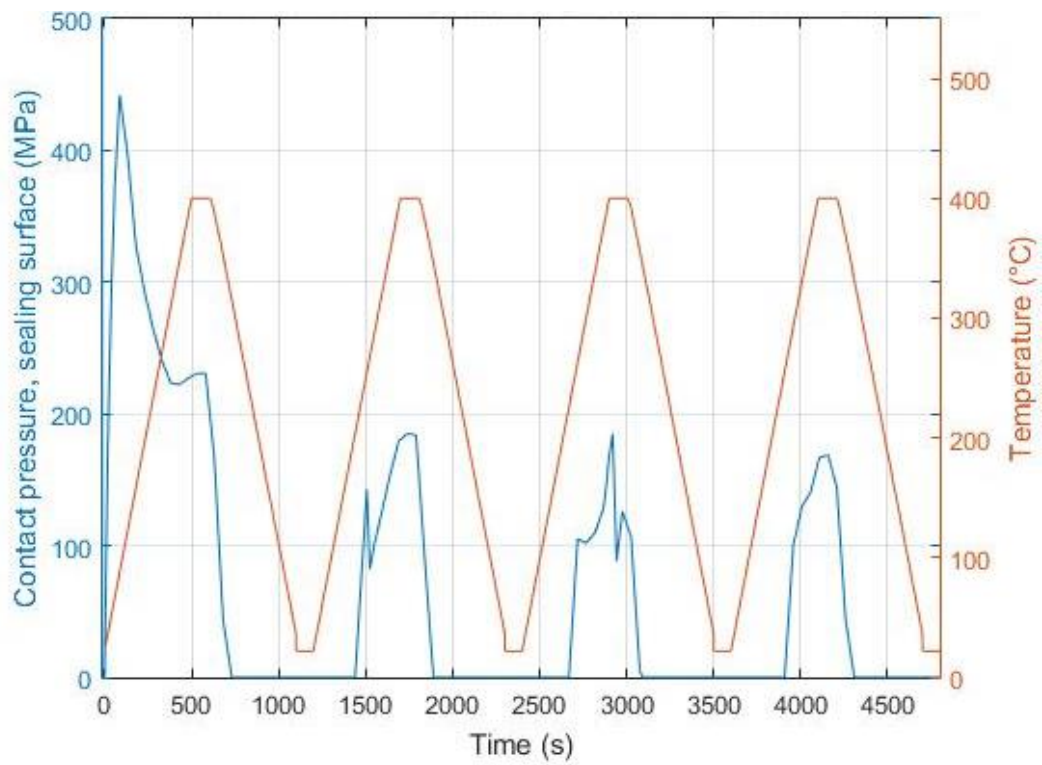


Figure 37: Load 2, Proprietary connection, K55, sealing surface contact pressure.

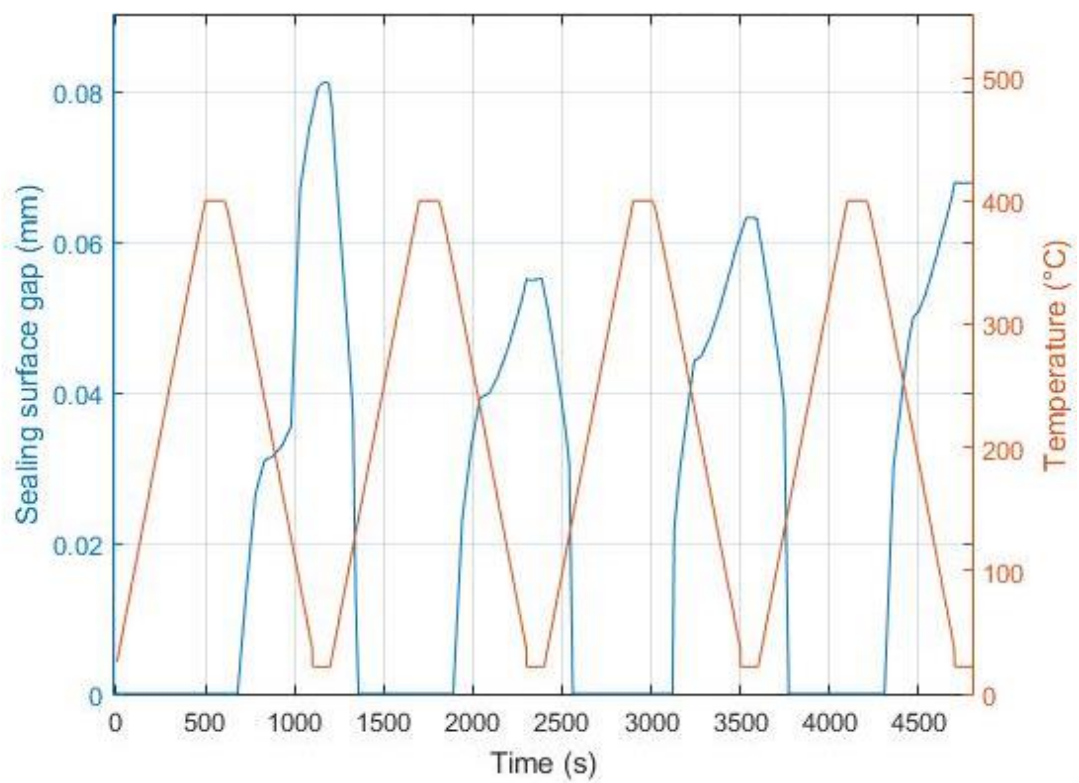


Figure 38: Load 2, Proprietary connection, K55, sealing surface gap.

### 4.3 Results for connection type 1, API BTC, grade L80

Stress and strain distribution in the connection is identical to the K55 grade but of different magnitude since the tensional and compressional strength of the N80 grade is greater than K55.

#### 4.3.1 Load case 1, API BTC, L80

The axial forces are of greater magnitude than the forces in the K55 casing. The L80 material is stressed far beyond the yielding point and is heavily plastically deformed like the K55 casing.

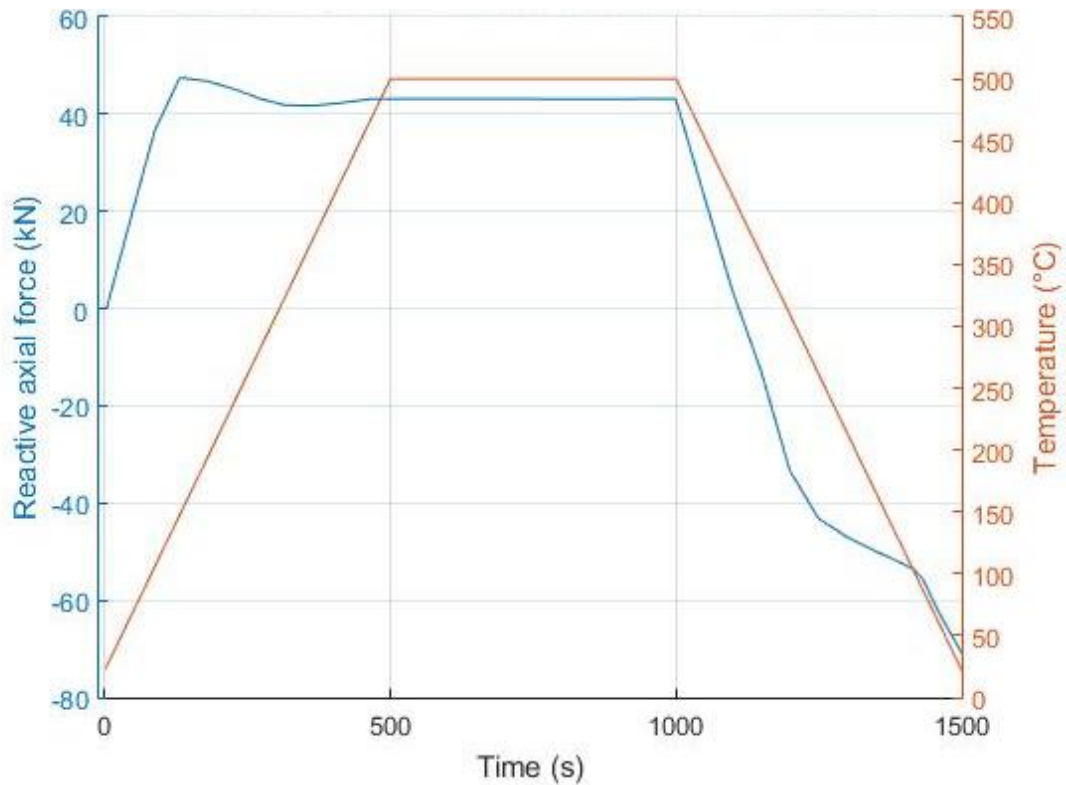


Figure 39: Figure 40, API BTC, N80, reactive axial force, load 1.

#### 4.3.2 Load case 2, API BTC, L80

Again the results are similar to the results for the K55 material and the cyclic load case does not highlight any advantages of stronger L80 material over K55. It can though be observed that tensional forces do not increase as much between load-cycles as K55 which indicates less strain hardening.

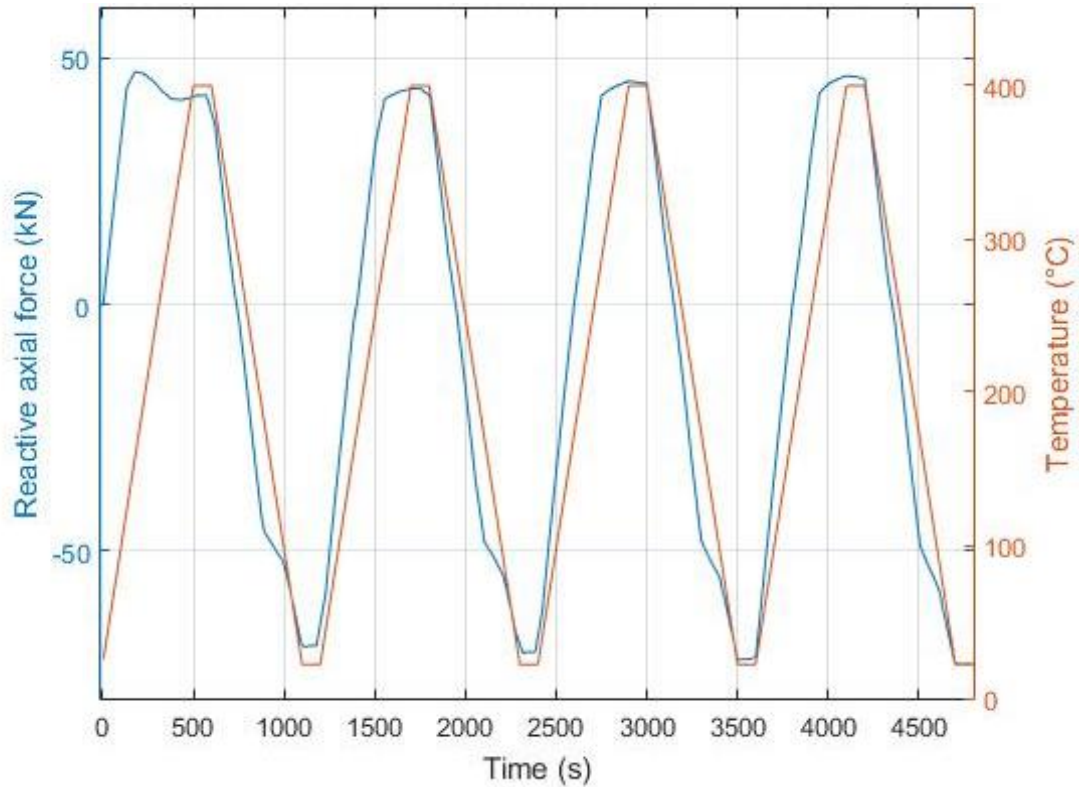


Figure 41: API BTC, N80, reactive axial force, load 2.

#### 4.4 Results for connection type 2 (Proprietary connection), grade L80

The same simulation was carried out for the proprietary connection from grade L80. Stress and strain distribution in the couplings are identical to the proprietary connection of K55 class but as for the API BTC connection of different magnitude is due to different material properties. The material is in all load cases heavily plastically deformed and the metal to metal seal is as vulnerable to plastic deformation as on the K55 coupling.

##### 4.4.1 Load case 1, Proprietary connection, L80

Figure 42 presents the reactive axial force. The results are identical to the K55 results but forces are of greater magnitude. The material is heavily plastically deformed and advantages of stronger material not observable.

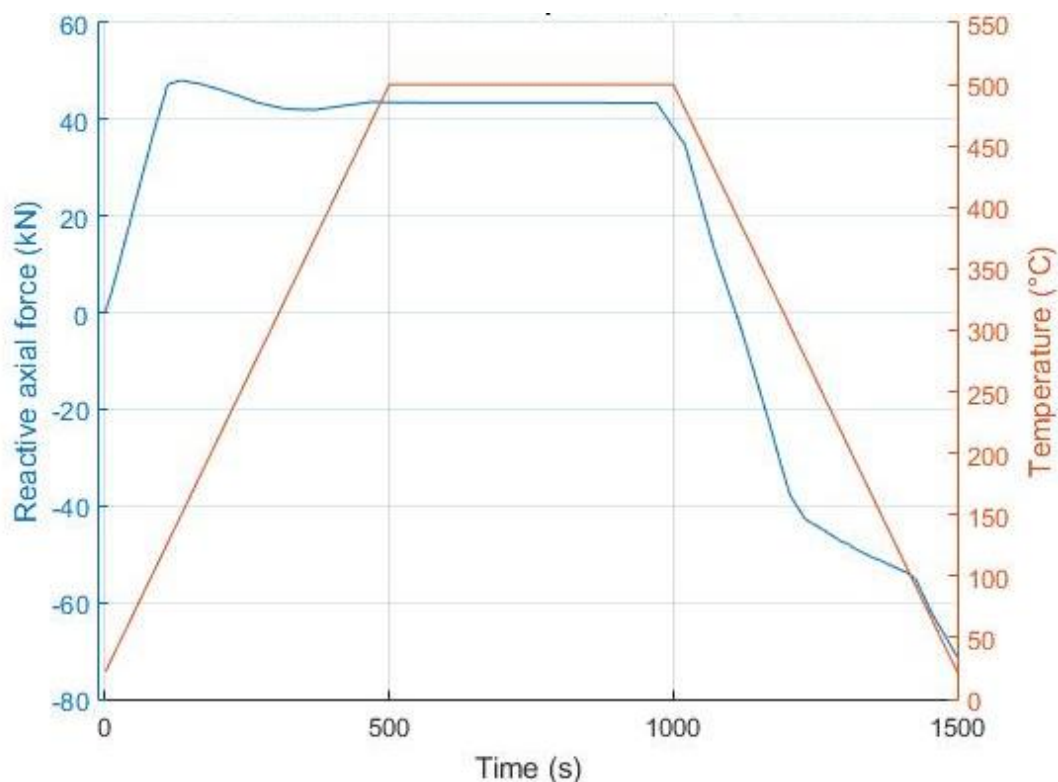


Figure 42: Proprietary connection, L80, reactive axial force, load case 1.

Figure 43 presents the sealing surface contact pressure. The L80 material shows no advantages over the K55 material regarding the integrity of the sealing surface.

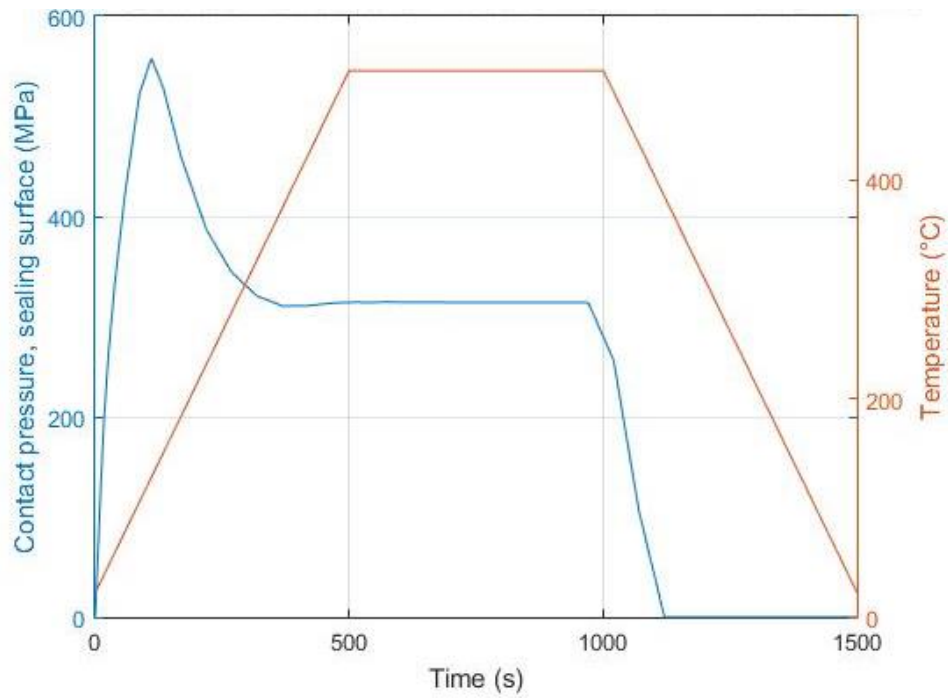


Figure 43: Proprietary connection, L80, sealing surface contact pressure.

#### 4.4.2 Load case 2, proprietary connection, L80

Figure 44 displays the reactive axial force for the cyclic load case.

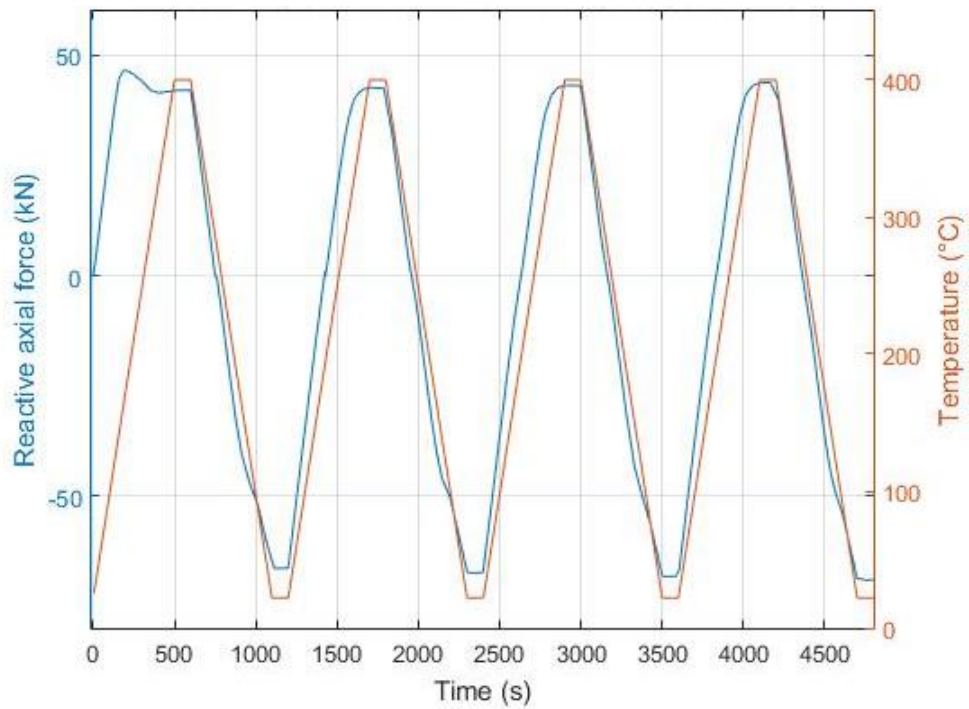


Figure 44: Proprietary connection, L80, reactive axial force, load case 2.

Just like for the conventional BTC connection, strain hardening appears to be less than in the K55 proprietary connection cyclic load case.

Figure 45 displays the sealing surface contact pressure for the cyclic load case.

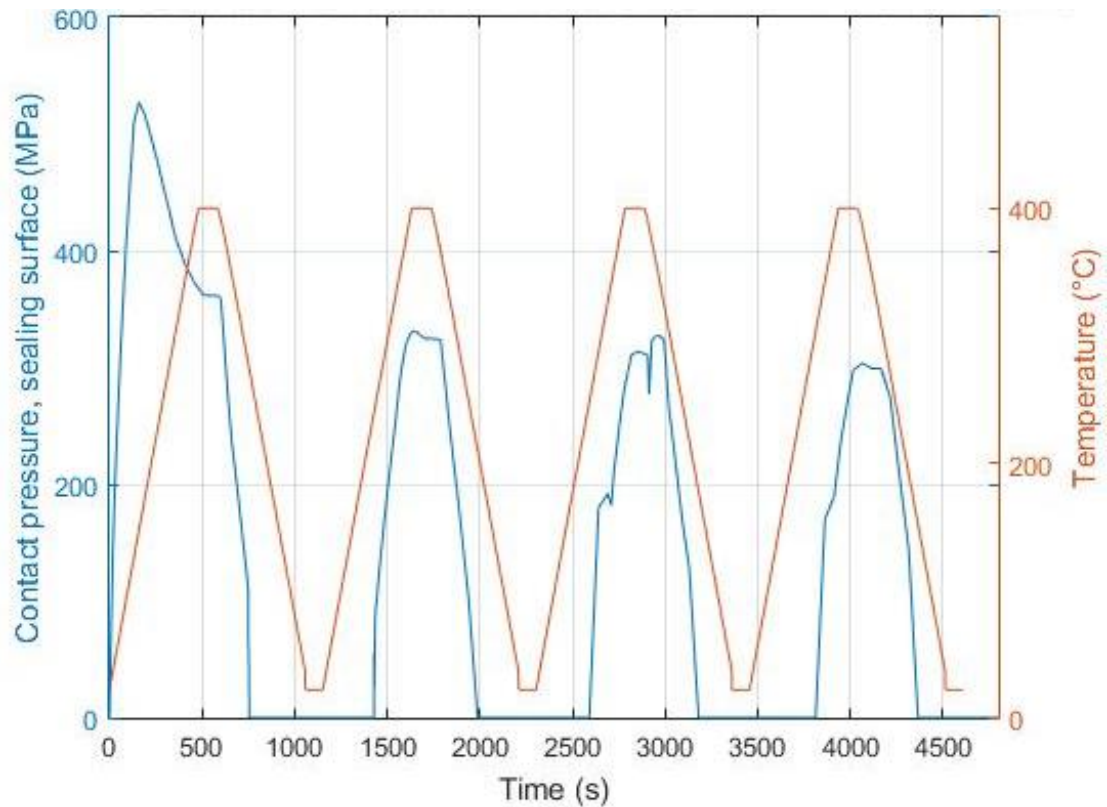


Figure 45: Proprietary connection, L80, sealing surface contact pressure, load case 2.

Figure 46 presents the sealing surface gap for the cyclic load case. The gap increases in every load cycle due to hardening of the material and results do not indicate any advantages over grade K55.

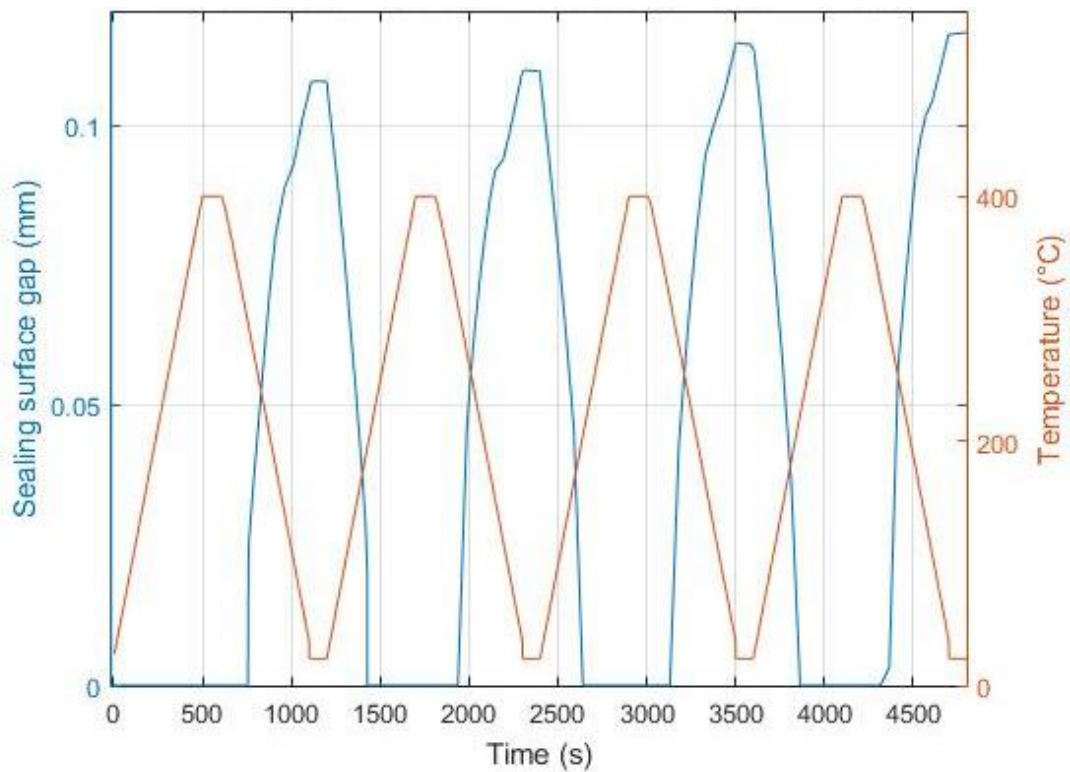


Figure 46: Proprietary connection, L80, sealing surface gap.

This research does not reveal any advantages of the use of higher strength material for the casing connection. The higher strength L80 casing connection appears to be as vulnerable as the K55 coupling for vast the axial loads driven by the restricted thermal expansion.

The L80 casing coupling is plastically deformed at similar temperature as the K55 coupling and the metal to metal seal proprietary connection shows no advantages over the K55 metal to metal connection. If the casing is able to endure more than one load cycle the metal to metal seal can't be assumed to be leak tight.



## 4.5 Casing string in pretension

As mention earlier, industry experts have indicated that applying pretension on casing strings while cementing might decrease plastic deformation due to restricted thermal expansion [27].

### 4.5.1 Pretension, API-BTC, K55

In Figure 47 the reactive axial forces and temperature are displayed. The casing is pulled in axial direction for the first 500 seconds at constant temperature and is then fixed throughout the thermal load-cycle. The tensional load applied approaches the yielding point of the material at initial temperature.

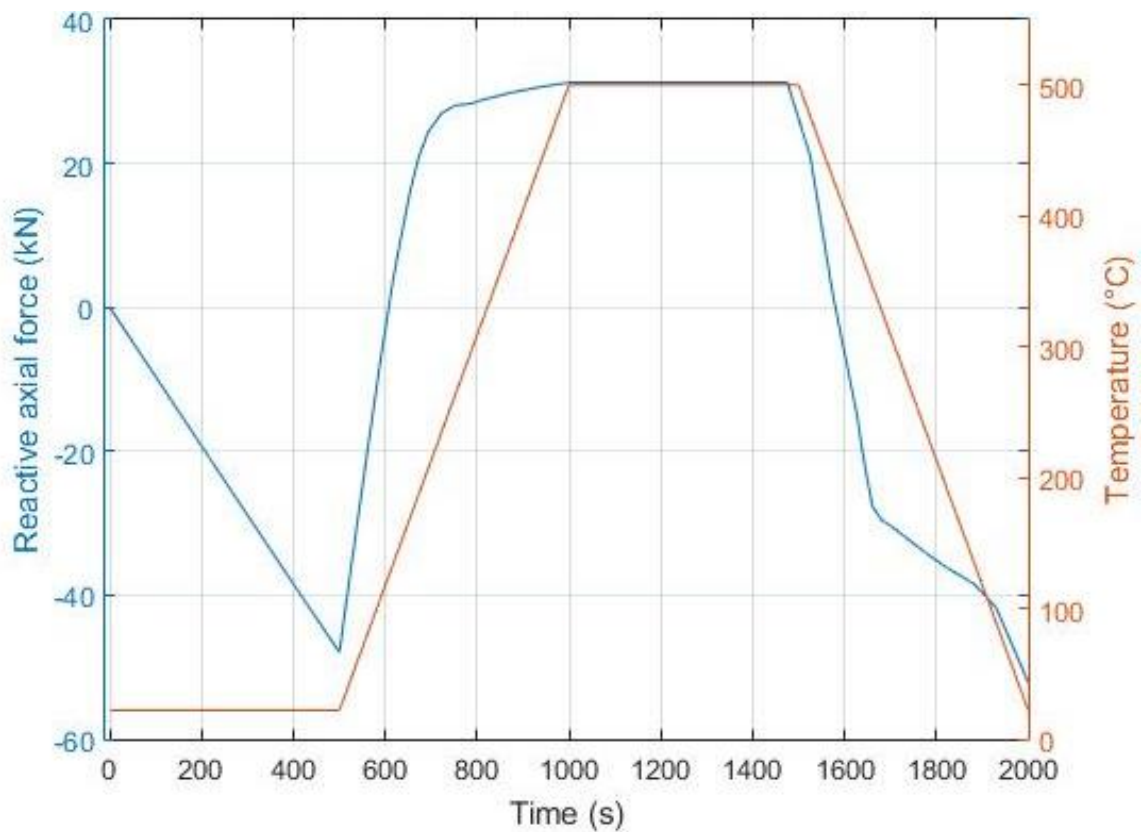


Figure 47: API-BTC, K55 in tension when thermal load is applied.



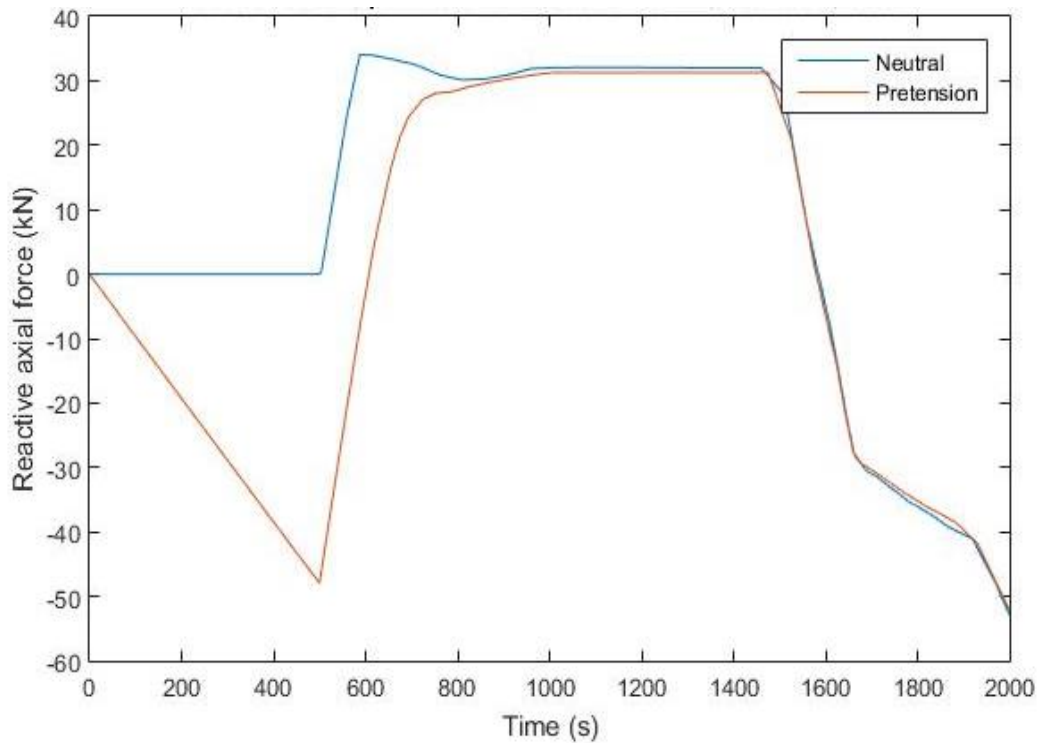


Figure 48: API-BTC, K55, pretension and neutral when thermal load is applied.

The casing string cemented in pretension is clearly plastically deformed at higher temperature than the casing string which is fixed in neutral stress state as presented in Figure 48.

The pre-stressed casing string is however heavily plastically deformed and the axial forces and deformation at the end of the load cycle where the material has been cooled back to initial temperature are not lesser than the forces in the neutral casing string.

The advantages of this technique for the extreme load examined are not supported by this research but it can though be concluded that this method is useful for lower temperature setting where plastic deformation might be reduced or even avoided by applying pretension. The neutral casing material is plastically deformed between 150 and 180°C while the pre-stressed material is plastically deformed around 220°C. This difference can be significant under some circumstances.

#### 4.6 Comparison, conventional conditions

As mentioned conventional geothermal conditions pose a great challenge for a casing string. In order to highlight further the extent of the load a casing coupling in a deep geothermal well experiences a load case for a casing coupling at conventional conditions was analyzed for comparison. Temperature in a conventional high temperature well is generally between 200-300°C. The temperature chosen for the comparison was based on measured wellhead temperature at Reykjanes.

The load is applied on a premium connection where all constraints and material properties are identical to the main study.

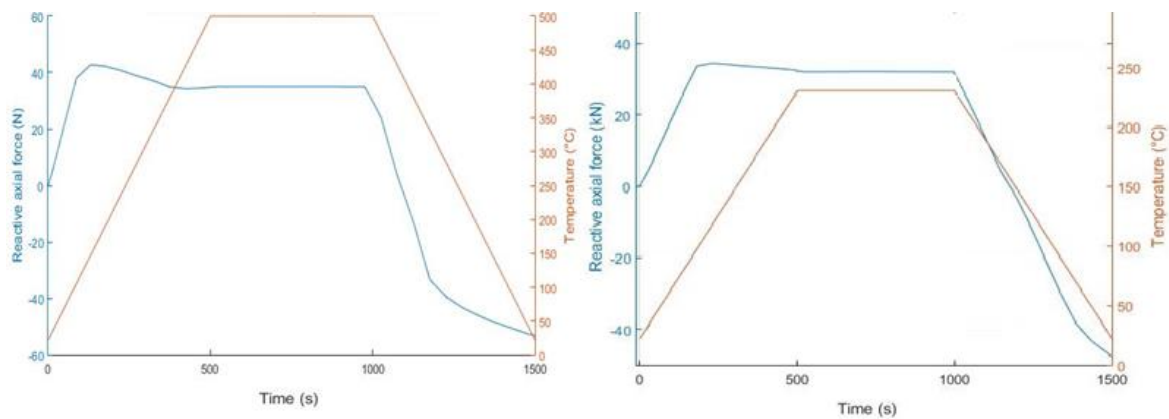


Figure 49, Comparison, Premium connection axial force.

In Figure 49 which is a comparison between single load cycles at extreme conditions to the left and conventional conditions to the right it can clearly be observed that the material is plastically deformed in compression in both cases. The difference is in the magnitude of the deformation as the material hardens far more in the extreme load case, it is compressed more and the connection shortens more which causes massive plastic deformation in the first load cycle when the thermal load decreases and the material contracts. Minor plastic deformation is present in the conventional load case but it is limited to the first thread on the coupling.

## **5 Conclusions and discussions**

### **5.1 Conclusions**

The case study covers the restricted thermal expansion load of two casing connections, one, API BTC proposed for the IDDP production casing and the other, a proprietary connection defined by the author with a metal to metal sealing surfaces which has been considered a promising option for geothermal setting. This study emphasizes the most severe load cases and conditions a casing string faces in a deep geothermal well.

The results of the case study indicate that the structural integrity of a threaded casing can't be ensured under the extreme thermal load expected in a deep well constructed for extraction of supercritical fluids from the bottom of a geothermal reservoir.

The threaded casing couplings are so heavily plastically deformed that it can be assumed that it is highly unlikely that a threaded casing string is able to endure a single load cycle and still provide the seal and structural support it is intended to provide. Furthermore, the results do not reveal any advantages of using higher grade casing material for examined conditions.

Regarding a connection with a metal to metal seal, it has been illustrated how the connection and sealing surfaces are heavily compressed and plastically deformed in the first load cycle. As soon as cooling of the proprietary connection from maximum temperature begins, the sealing surfaces are separated and can no longer provide proper sealing. The sealing surface gap which is zero before the thermal load is introduced increases between load steps which indicates that if the connection is able to endure multiple load cycles where plastic deformation occurs the sealing ability worsens between cycles. The sealing surface transfers the axial compressional forces but the threads bear the tensional forces which after one load cycle are similar to the tensional forces in the conventional API-BTC connection. This research indicates that the advantages of a metal to metal proprietary connection over conventional connection are minimal if any under the inspected loads.

The pre-stressed casing installation does not seem to be beneficial for extreme conditions like those expected in deep geothermal wells. It can nevertheless be concluded that controlled pretension of a casing string might be advantageous and can reduce stress and help avoid yield in a casing under conventional geothermal conditions.

## **5.2 Discussions**

In this study the main focus is on the loads rendered by restricted thermal expansion. This is as mentioned in the text only one of many loads a casing has to endure, but by far the most intense. This study indicates that the advantages of higher grade (API 5CT) material is not advantageous and the metal to metal seal coupling does not provide better sealing than conventional couplings. It has to be taken into account that some material properties are neglected and the material model includes assumptions. The API casing material grades are very widely defined and many types of material can fall into the same API grade, particularly the lower grades where requirements are lesser. Accurate test data which represents the material properties of the grades is therefore not available and scarcity of material data potentially the greatest limitation of this research.

Research has indicated that creep and stress relaxation in the casing string might be an important contributor to casing failure in geothermal wells [23]. The casing string is compressed and plastically deformed and stress in the material is relaxed with time. The deformation is permanent and if stress has been relaxed significantly this might cause plastic deformation to happen at higher temperature during cooling and greater tensional load if a well has to be quenched. This would have been interesting and is an important factor but again material data was not available to include time dependent properties of the casing material examined.

Finding the optimum casing connection and material for extreme geothermal conditions is a large task. Many options have been discussed, options like material with low or no thermal expansion, complex wellheads which allow the developer to service the well to some extent without stopping flow from the well and casing connections which do not transfer stress are among choices which have been on the table.

Casing made from high performance materials is not available at acceptable price and the complex wellheads only resolve part of the problem. Downhole service is very likely needed at some point during the wells operational life and a complex wellhead does therefor just address a part of the problem.

It is the author's opinion that a casing connection which provides reliable sealing and does not transfer axial forces between members of the casing string is a promising solution to the connection problem and other potential problems like buckling of the casing string which might render a well inoperable in a severe case.

Such connection is though not available yet and the design would be an exciting challenge which might revolve geothermal well design if successful.

Another option, a well-known established method and widely used, is probably the most straight-forward solution, the use of butt-welded casing joint for all the casing programs. A welded connection is resilient and offers connection efficiency of 100% in both tension and compression. The downside of the welded solution is longer trip in time but in the context of the construction time of a deep well the trip in time is a negligible factor.

It can be concluded from the results of this study that while the extraction of supercritical fluids from naturally occurring geothermal resources is still at experimental stage and the use of premium materials with low thermal expansion is not a possibility the best threaded option might be K55 BTC.

The simplest options often tend to be overlooked but while threaded solutions which can endure more are not available it is the author's opinion that butt-welded casing joints and alternative well design should be considered for imminent deep geothermal wells.

## 6 Bibliography

- [1] G.Ó.Friðleifsson, W.A.Elders and A.Albertsson, "The concept of the Iceland deep drilling project," *Geothermics*, vol. 49, pp. 2-8, 2014.
- [2] H. Hole, "Geothermal well design-Casing and wellhead," in *Petroleum engineering summer school workshop 26*, 2008.
- [3] J. Xie and G. Tao, "Analysis of Casing Connections Subjected to," in *SIMULIA Customer Conference*, Edmonton, 2010.
- [4] M. Dickison and M. Fanelli, "IGA," IGA, February 2004. [Online]. Available: [http://www.geothermal-energy.org/what\\_is\\_geothermal\\_energy.html](http://www.geothermal-energy.org/what_is_geothermal_energy.html). [Accessed 29 April 2015].
- [5] Orkustofnun, "Orkustofnun," August 2015. [Online]. Available: <http://www.orkustofnun.is/orkustofnun/hafa-samband/jardhitaaudlindin-a-islandi/flokkun-jardhitakerfa/>.
- [6] G. Axelsson, "PRODUCTION CAPACITY OF GEOTHERMAL SYSTEMS," Orkustofnun, Reykjavík, 2008.
- [7] Orkustofnun, "Orkustofnun, Jarðvarmavirkjanir," Orkustofnun, 2015. [Online]. Available: <http://os.is/jardhiti/jardhitanotkun/jardvarmavirkjanir/>. [Accessed 6 5 2015].
- [8] R. DiPippo, *Geothermal Power Plants: Principles, Applications, Case Studies and Environmental Impact*, Elsevier, 2008.
- [9] M.-C. S. Arriga and F. S. V, "DEEP GEOTHERMAL RESERVOIRS WITH WATER AT SUPERCRITICAL CONDITIONS," in *Thirty-Seventh Workshop on Geothermal Reservoir Engineering*, 2012.
- [10] G. Friðleifsson, W. Elders and A. Albertsson, "The concept of the Iceland deep drilling project," *Geothermics*, vol. 48, 2014.
- [11] G. Ó. Friðleifsson and W. A. Elders, "The Science Program of the Iceland Deep Drilling Project (IDDP): a Study of Supercritical Geothermal Resources," in *Proceedings World Geothermal Congress 2010*, 2010.

- [12] Pálsson, Hólmgeirsson, Guðmundsson, Bóasson, Ingason, Sverrisson and Thórhallsson, "Drilling of the well IDDP-1," *Geothermics*, no. 49, pp. 23-30, 2014.
- [13] K. Ingason, A. B. Árnason, H. Á. Bóasson, H. Sverrisson, S. Kjartan Ö and Þ. Gíslason, "IDDP-2, Well design," in *World Geothermal Congress 2015*, Melbourne, 2015.
- [14] M. Merliahad, B. Giacomel and K. Sakura, "Casing Connection Selection for Geothermal Applications Using New Input From HPHT," in *Proceedings World Geothermal Congress 2015*, Melbourne, 2015.
- [15] J. L. Dossett and H. E. Boyer, *Practical Heat Treating*, second edition, Ohio: ASM International, 2006.
- [16] B. Juneja, *Fundamentals of Metal Forming Process*, Delhi: New Age International, 2010.
- [17] Budynas and Nisbett, *Shigley's Mechanical Engineering Design*, Eight Edition, McGraw-Hill, 2008.
- [18] W. B. Bickford, *Mechanics of Solids, concepts and applications*, Irwin, 1993.
- [19] A. P. Institute, *API Specification 5CT, Eighth Edition*, Washington D.C.: API Publishing Services, 2005.
- [20] S. Þórhallsson, "CORROSION IN GEOTHERMAL WELLS AND INSTALLATIONS," in *Short Course on Geothermal Development and Geothermal Wells*, Santa Tecla, 2012.
- [21] S. Thórhallsson, M. Matthíasson, T. Gíslason, K. Ingason, B. Pálsson and G. Ó. Fridleifsson, "IDDP feasibility report part 2," 2003.
- [22] S. Thorhallsson, B. Pálsson, S. Hólmgeirsson, K. Ingason, M. Matthíasson, H. Á. Bóasson and H. Sverrisson, "Well design and drilling plans of the Iceland Deep Drilling Project (IDDP)," in *World Geothermal Congress 2010*, Bali, 2010.
- [23] Maruyama, Tsuru, Ogasawara, Inoue and Peters, "An Experimental Study of Chasing Performance Under Thermal Cycling Conditions," *SPE Drilling Engineering*, vol. 5, no. 2, pp. 156-164, 1990.

- [24] G. Gaboulde and J. P. Nguyen, *Drilling Data Handbook*, Paris: Editions TECHNIP, 2006.
- [25] G. S. Kaldal, M. Þ. Jónsson, H. Pálsson and S. N. Karlsdóttir, "Thermal and structural analysis of the casing in a high temperature geothermal well during discharge," in *Thirty seventh workshop on geothermal reservoir engineering*, 2012.
- [26] G. S. Kaldal, M. Þ. Jónsson, H. Pálsson, S. N. Karlsdóttir and I. Ö. Þorbjörnsson, "Load history and buckling of the production casing in a high temperature geothermal well," in *Thirty-Sixt Workshop on Geothermal Reservoir Engineering*, 2011.
- [27] S. Þórhallsson, Interviewee, *Discussion about drilling technology at Orkugarður*. [Interview]. 28 5 2015.
- [28] C. Teodoriu and G. Falcone, "FATIGUE LIFE PREDICTION OF A BUTTRESS CASING CONNECTION EXPOSED TO," in *Thirty-Third Workshop on Geothermal Reservoir Engineering*, Stanford, 2008.
- [29] S. Moaveni, *Finite Element Analysis, Theory and Application with ANSY*, New Jersey: Pearson Education, Inc., 2003.
- [30] J. Peiro and S. Sherwin, "FINITE DIFFERENCE, FINITE ELEMENT," in *Handbook of Materials Modeling*, Springer, 2005, pp. 1-32.
- [31] O. Zienkiewicz and R. Taylor, *The Finite Element Method, Volume 1 the Basis*, Butterworth Heinmann, 2000.
- [32] *European standard, EN 13445-2(2002),Unfired pressure vessels - Part 2: Materials*, 2002.
- [33] *EN 10216-2, seamless steel tubes for pressure purposes. technical delivery conditions.*, 2004.
- [34] J. Chen, B. Young and B. Uy, "Behavior of high strength structural steel at elevated," *Journal of Structural Engineering, ASCE*, pp. 1948-1954, 2006.
- [35] S. A. o. N. Zealand, *Code of Practice for Deep Geothermal Wells*, Wellington: Stanard Association of New Zealand, 1991.
- [36] I. B. Friðleifsson, "Historical aspects of geothermal utilization in Iceland," *Orkustofnun, Reykjavik*, 1999.



